European Journal of Medicinal Chemistry 127 (2017) 318–333

Contents lists available at ScienceDirect

European Journal of Medicinal Chemistry

journal homepage: http://www.elsevier.com/locate/ejmech

Research paper

# Rational design, synthesis, and evaluation of novel 2,4-Chloro- and Hydroxy-Substituted diphenyl Benzofuro[3,2-*b*]Pyridines: Non-intercalative catalytic topoisomerase I and II dual inhibitor

Seojeong Park [a, 1], Til Bahadur Thapa Magar [b, 1], Tara Man Kadayat [b], Hwa Jong Lee [a], Ganesh Bist [b], Aarajana Shrestha [b], Eung-Seok Lee [b, *], Youngjoo Kwon [a, **]

[a] College of Pharmacy, Graduate School of Pharmaceutical Sciences, Ewha Womans University, Seoul 120-750, Republic of Korea
[b] College of Pharmacy, Yeungnam University, Gyeongsan 712-749, Republic of Korea

ARTICLE INFO

*Article history:*
Received 28 September 2016
Received in revised form
28 November 2016
Accepted 1 January 2017
Available online 2 January 2017

*Keywords:*
2,4-chloro- and hydroxy-substituted diphenyl benzofuro[3,2-*b*]pyridines
Dual topoisomerase I and II inhibition
Antiproliferative activity
Non-intercalative catalytic inhibiton
Anticancer agent

ABSTRACT

Novel series of conformationally constrained 2,4-chloro- and hydroxy-substituted diphenyl benzofuro [3,2-*b*]pyridines were rationally designed and synthesized. Their biological activities were evaluated for topoisomerase I and II inhibitory activity, and antiproliferative activity against several human cancer cell lines for the development of novel anticancer agents. Most of the compounds with phenol moiety at 4-position of central pyridine exhibited significant dual topoisomerase I and II inhibitory activities, and strong antiproliferative activity in low micromolar range. Structure activity relationship study suggested that phenol moiety at 4-position of the central pyridine regardless of chlorophenyl moiety at 2-position of the central pyridine has an important role in dual topoisomerase inhibitory activity as well as antiproliferative activity. For investigation of mode of action for compound **14** which displayed the most strong dual topoisomerase I and II inhibitory activity and antiproliferative activity against HCT15 cell, we performed cleavable complex assay, band depletion assay, comet assay, and competitive EtBr displacement assay. Compound **14** functioned as non-intercalative catalytic topo I and II dual inhibitor. In addition, compound **14** induced apoptosis in HCT15 cells through increase of Bax, decrease of Bcl-2 and increase of PARP cleavage.



## 1. Introduction

It has been generally considered that caner is a very complicated disease caused by multiple pathogenic factors. The characteristics of cancer are an accelerated rate of tumor cell proliferation and numerous genetic (inherent) and/or epigenetic mutations to extend their survival [1]. Despite of diverse and heterogeneous characters of tumors, all types of tumors have in common the accelerated cell proliferation rate which is positively related to the overexpression of DNA topoisomerase (topo) in tumors [1,2].

Human DNA topo, a nuclear enzyme, is the key component of the cell which can solve all topological problems of DNA associated with several vital cellular processes like DNA replication, transcription, recombination, repair, chromatin assembly and chromosome segregation [3,4]. Since the discovery of topo by J. C. Wang in 1971, it has been shown to be one of the promising molecular targets of anticancer agents [5,6]. There are two types of human DNA topo; one is topo I which makes DNA single strand cleavage at a time. The other is topo II which induces concurrent cleavage on DNA double strands. During DNA cleavage process by topo I or topo II, the covalent bond is transiently formed between topo and DNA giving rise to DNA-topo cleavable complex followed by going back to DNA religation which peruses DNA relaxation or unwinding processes to solve DNA topological problems [7]. Those compounds, which stabilize the cleavable complex by forming topo-DNA-compound ternary complex leading to disturbance on this specific religation step in the catalytic cycle of topo function mechanism, are termed as topo poisons. On the other hand, compounds, which function on the other steps beside prevention from the religation step, are named as topo catalytic cycle inhibitors. Just as predicted in the nomenclature, topo poisons generate more

* Corresponding author.
** Corresponding author.
*E-mail addresses:* eslee@ynu.ac.kr (E.-S. Lee), ykwon@ewha.ac.kr (Y. Kwon).
[1] Authors are equal contributors.

http://dx.doi.org/10.1016/j.ejmech.2017.01.003
0223-5234/

detrimental DNA truncation and severe genotoxicity [8,9]. At the present, camptothecin, topotecan, irinotecan, etoposide, and teniposide are under clinical use as topo-targeting anticancer drugs. Although extensive investigation on topo inhibitors in the last four decades has offered several potent anticancer drugs, they have undesirable side effects and other limitations such as an induction of secondary malignancy during medication [10]. Further investigation is needed for the development of better topo-targeting anticancer agent. Depending upon the cell types, the expression of topo I and topo II is markedly different. Topo I is highly expressed in colon cancer cell lines [11], while topo II expression is high in breast and ovarian cancer cell lines [12]. It is also observed that the time-course of topo I and topo II expression differs during cell cycle. Topo I expression is relatively constant throughout the cell cycle, whereas topo II expression is maximum at S phase [13]. Either of the enzyme expression is sufficient for cell division and the resistance to topo I inhibitor is developed due to concomitant increase in topo II expression and vice versa [14]. Therefore, dual topo I and II inhibitors have the advantage and the interest of medicinal chemists is growing towards research for the development of dual topo I and II-targeting anticancer drugs [15,16].

Many researchers have reported that several natural and synthetic benzofuran containing compounds exhibit potent anticancer activities via wide variety of mechanisms including aromatase inhibition [17], hypoxia-inducible factor 1-alpha (HIF-1α) inhibition [18], topo inhibition [19], farnesyltransferase inhibition [20], proto-oncogene serine/threonine-protein kinase (Pim-1) inhibition [21], HDAC inhibition [22], GSK-3β inhibition [23], and mTOR inhibition [24]. Moreover, it has been reported that halogen containing compounds improve the drug-target binding affinity by forming halogen bonds [25–27]. Especially, chlorination of 2- or 4-phenyl ring increased the topo I and topo II inhibitory activity as well as antiproliferative activity against several human cancer cell lines [28,29]. Furthermore, hydroxylation is important for the formation of H-bond leading to enhanced topo I and II inhibitory activity and antiproliferative activity [30]. In addition, previously reported conformationally constrained 2-phenol-4-phenylbenzofuro[3,2-*b*] pyridine (compound **I**, Fig. 1) which contains benzofuran moiety displayed dual topo I and topo II inhibitory activity [31]. It has been considered that rigid structure has planar configuration and less conformational entropy facilitating compound to be fitted more efficiently into the active site of target enzyme [32].

On the basis of previous reports and results, we introduced conformationally rigid novel benzofuran moiety bearing chloride and hydroxyl functionality at 2- or 4-phenyl ring, which expected to display dual topo I and topo II inhibitory activity as well as to improve their biological activities. The strategy for design of 2,4-chloro- and hydroxy-substituted diphenyl benzofuro[3,2-*b*]pyridines is shown in Fig. 2. Benzofuropyridine is the novel rigid moiety first discovered in our research group having dual topo I and topo II inhibitory activity, and antiproliferative activity against several human cancer cell lines. In this study, we have designed and synthesized eighteen novel series of benzofuro[3,2-*b*]pyridines possessing 2′-, 3′-, or 4′-chlorophenyl and 2′-, 3′-, or 4′-phenol moiety at 2- and 4-position of the central pyridine ring as shown in Fig. 3.

## 2. Results and discussion

### 2.1. Synthetic chemistry

As illustrated in Scheme 1, benzofuro[3,2-*b*]pyridines containing chlorophenyl or phenol moiety at 2- and 4-position of central pyridine were synthesized in three steps based on the previously reported methods [31,33]. At first, reaction of appropriate aryl methyl ketones **1** (R = **a-f**) with equivalent amount of iodine in pyridine for 3 h at 140 °C generated corresponding pyridinium iodide salts **2** (R = **a-f**) in 52.2–93.0% yield. Secondly, benzofuran-3(*2H*)-one intermediates **5** ($R^1$ = **a-f**) were synthesized using benzofuran-3(*2H*)-one (**3**) and aryl aldehyde **4** ($R^1$ = **a-f**) as starting material in the presence of activated, basic aluminum oxide and methylene chloride for 3 h at 25 °C. Total six benzofuran-3(*2H*)-one intermediates **5** ($R^1$ = **a-f**) were synthesized in the yield of 51.0–81.6%. Finally, treatment of pyridinium iodide salts **2** (R = **a-f**) and benzofuran-3(*2H*)-one intermediates **5** ($R^1$ = **a-f**) in the presence of $NH_4OAc$ and glacial acetic acid for 12–24 h at 100 °C afforded the corresponding 2,4-chloro- and hydroxy-substituted diphenyl benzofuro[3,2-*b*]pyridines (**6**–**23**) via modified Kröhnke pyridine synthesis method [34] in the yield of 8.9–36.5%. Yield (%), purity (%), retention time (min) obtained from HPLC analysis, and melting point (°C) of each of synthesized compounds are summarized in Table S1 (Supplementary Data).

### 2.2. Topoisomerase I and II inhibitory activity

We measured the extent of topo I or II-mediated conversion of supercoiled DNA to relaxed DNA in the absence and presence of the prepared 2,4-chloro- and hydroxy-substituted diphenyl benzofuro [3,2-*b*]pyridines (**6**–**23**) as shown in Fig. 4, and their % inhibitory activities are summarized in Table 1. Camptothecin and etoposide, selective topo I and II inhibitors, respectively, were used as positive controls. Inhibitory activities were evaluated at 100 μM in which compounds showing more than 30% inhibitory activity were further examined at 20 μM.

#### 2.2.1. Topoisomerase I inhibitory activity

As shown in Fig. 4A, majority of the compounds displayed the considerable to significant topo I inhibitory activity. Among the tested compounds, **14** possesses the most significant topo I inhibitory activity (95.6% at 100 μM, 47.9% at 20 μM) which is more active than a positive control, camptothecin (59.0% at 100 μM, 34.1% at 20 μM). Compounds **8**–**14** containing 2′-, 3′-, or 4′-chlorophenyl at 2-position and 2′-, 3′-, or 4′-hydroxyphenyl group at 4-position of central pyridine showed significant topo I inhibitory activity at both 100 μM and 20 μM concentrations. On the other hand, compounds **15**–**23** possessing 2′-, 3′-, or 4′-hydroxylpheny group at 2-poisition and 2′-, 3′-, or 4′-chlorphenyl group at 4-position of central pyridine showed moderate to significant topo I inhibitory activity (41.7%–87.5%) only at 100 μM.

#### 2.2.2. Topoisomerase II inhibitory activity

Compounds **6**–**14** containing 2′-, 3′-, or 4′-chlorophenyl at 2-position and 2′-, 3′-, or 4′-hydroxyphenyl group at 4-position of central pyridine displayed significant topo II inhibitory activity (82.9%–100%) as compared to etoposide (86.9%) at 100 μM. Especially, compound **14** with 4′-chlorophenyl at 2-position and 4′-hydroxyphenyl at 4-position of central pyridine showed the most potent topo II inhibitory activity of 100% (100 μM) and 59.8% (20 μM) which are more active than etoposide (86.9% at 100 μM, 34.2% at 20 μM). However, compounds **15**–**23** possessing 2′-, 3′-, or 4′-hydroxylpheny group at 2-poisition and 2′-, 3′-, or 4′-chlorphenyl group at 4-position of central pyridine did not show significant topo II inhibitory activity (0%–65.6% at 100 μM). Among the compounds **15**–**23**, compounds **15**, **16**, **17**, and **23** displayed comparable topo II inhibitory activity.

### 2.3. Antiproliferative activity

Three different human cancer cell lines were used for the evaluation of antiproliferative activity: human colorectal adenocarcinoma cell line (HCT15), human breast cancer cell line (T47D),

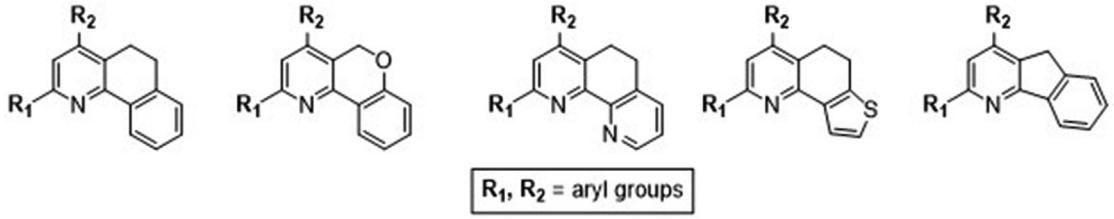


(a) Rigid analogs of 2,4,6-trisubstituted pyridines

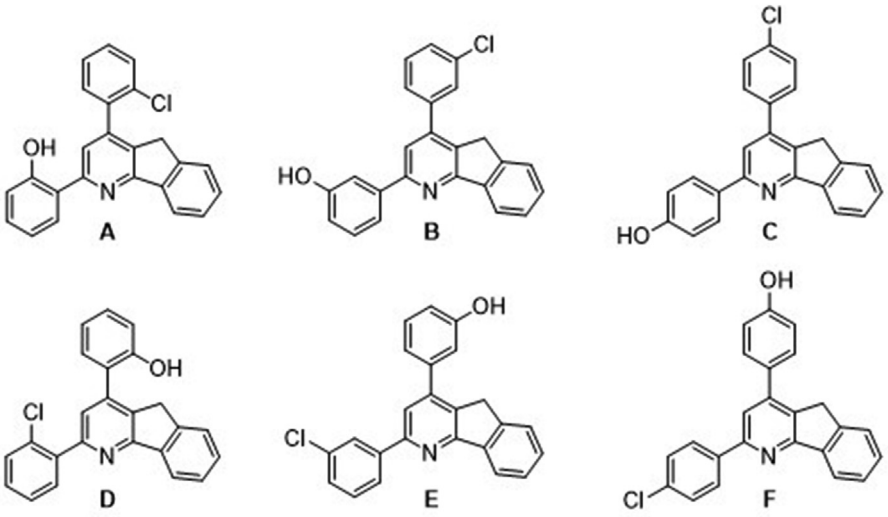


(b) Chloro- and hydroxy-substitued 2,4-diphenyl indenopyridines

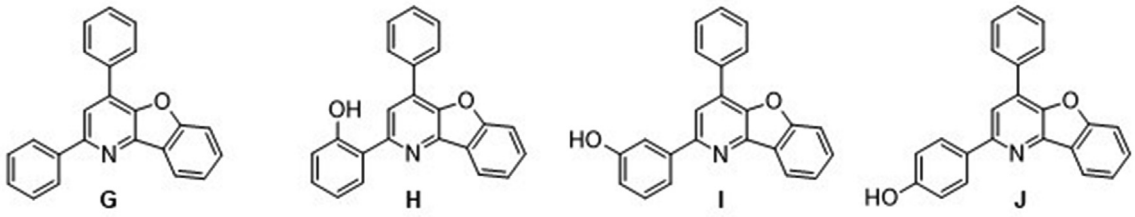


(c) 2-Phenyl- or 2-hydroxyphenyl-4-phenyl benzofuro[3,2-*b*]pyridines

**Fig. 1.** Structures of previously synthesized rigid analogs of (a) 2,4,6-trisubstituted pyridines, (b) Chloro- and hydroxy-substituted 2,4-diphenyl indenopyridines, and (c) 2-phenyl- or hydroxyphenyl-4-phenyl benzofuro[3,2-*b*]pyridines.

and human cervix tumor cell line (HeLa). $IC_{50}$ values determined for compounds **6**–**23** are listed in Table 1. Most of the compounds exhibited significant antiproliferative activity against tested cell lines. Among all the tested compounds, compound **6**, **7** and **10**–**15** displayed strong antiproliferative activity against HCT15 as compared to positive controls. Compound **7** showed the strongest antiproliferative activity (0.01 μM) especially against HCT15 which is 60, 540 and 100 fold more potent than positive controls camptothecin, etoposide, and adriamycin, respectively although the topo I and II inhibitory activity of compound **7** was less potent than compound **14**. The better antiproliferative activity of compound **7** with less topo I and II inhibitory than compound **14** reflected compound **7** is likely to have another targets related to cell proliferation process in cells. Compound **14** possessing excellent dual topo I and II inhibitory activity also showed strong antiproliferative activity against HCT15 cell line as compared to all three positive controls. All of the compounds except **8** which containing 2′-, 3′-, or 4′-chlorophenyl at 2-position and 2′-, 3′-, or 4′-hydroxyphenyl group at 4-position of central pyridine (compounds **6**–**14**) showed significant antiproliferative activity against all the tested cancer cell lines. However, more than half compounds (**17**, **18**, **21**, **22**, and **23**) which possessing 2′-, 3′-, or 4′-hydroxylpheny group at 2-poisition and 2′-, 3′-, or 4′-chlorphenyl group at 4-position of central pyridine (compounds **15**–**23**) did not displayed considerable antiproliferative activity. Among the compounds **15**–**23** only **15**, **16**, and **19** displayed significant antiproliferative activity against all the tested cancer cell lines. As illustrated by results of antiproliferative activity, compounds bearing phenol on 4-position of central pyridine ring showed stronger antiproliferative activity than those of bearing phenol on 2-position. In addition, antiproliferative activity was not depending on the position of chlorophenyl on 2-position of central pyridine ring.

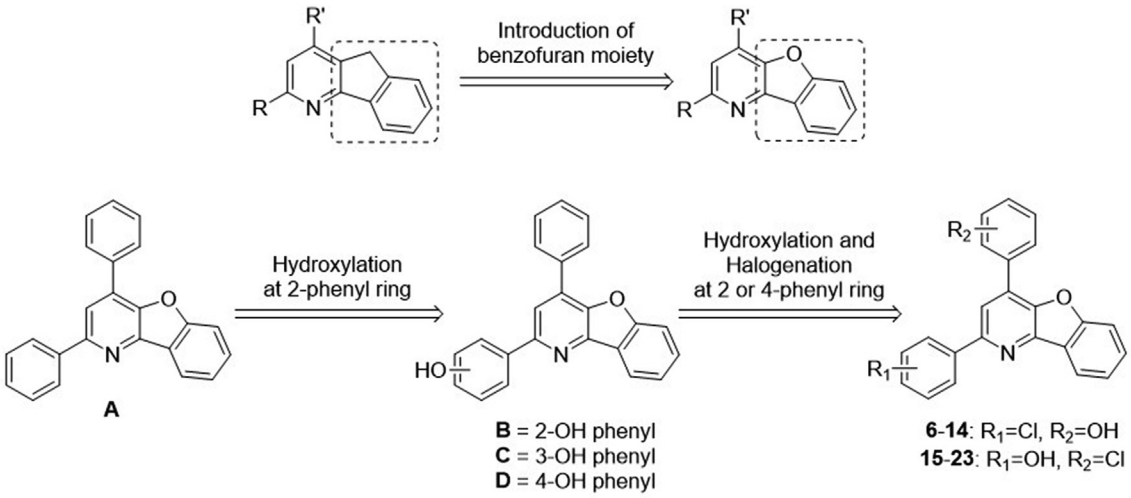


**Fig. 2.** Strategy for the design of 2,4-chloro- and hydroxy-substituted diphenyl benzofuro[3,2-*b*]pyridines.

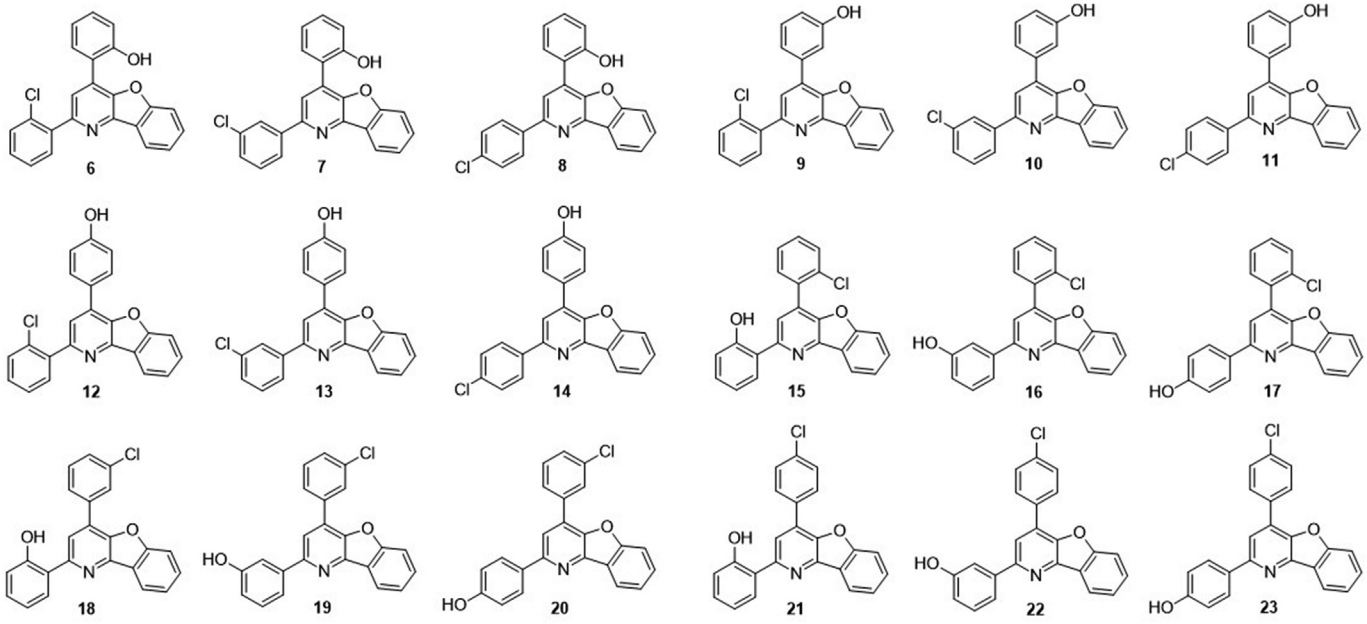


**Fig. 3.** Structures of the prepared 2,4-chloro- and hydroxy-substituted diphenyl benzofuro[3,2-*b*]pyridines.

### *2.4. Structure-activity relationship study (SAR)*

We performed the structure-activity relationship study utilizing the results of topo I and topo II inhibitory activity, and antiproliferative activity of 2- or 4-chlorophenyl-2- or 4-hydroxyphenyl-5*H*-indeno[1,2-*b*]pyridines (**A-F**), 2,4-diphenylbenzofuro[3,2-*b*]pyridines (**G**), 2-hydroxyphenyl-4-phenylbenzofuro[3,2-*b*]pyridines (**H-J**), and 2,4-chloro- and hydroxy-substituted diphenyl benzofuro[3,2-*b*]pyridines (**6**–**23**). Fig. 1 shows the structures of previously reported compounds and Table 2 summarizes the relative topo I and II inhibitory potencies of the representative compounds at 100 μM and 20 μM concentrations. Interestingly, replacement of conventional indenopyridine moiety (**A-F**) with 2,4-chloro- and hydroxy-substituted diphenyl benzofuro[3,2-*b*]pyridines (**6**–**23**) significantly enhanced the topo I and topo II inhibitory activity as well as antiproliferative activity. Relative potency of non-substituted compound **G** is very low as compared with hydroxyl or chloride substituted analogs. On the other hand, introduction of chloride functionality (**6**–**23**) on 2-hydroxyphenyl-4-phenylbenzofuro[3,2-*b*]pyridine derivatives (**H-J**) displayed mixed results. Among tested compounds in the current study, compounds **15**–**23** were obtained by introduction of 2′-, 3′-, or 4′-chloride at 4-phenylring of compounds **H-J**. Compounds **15** and **21** having 4-(2′-chlorophenyl) and 4-(4′-chorophenyl) moiety, respectively, showed better topo I and topo II inhibitory activity than respective non-chlorinated analog (**H**). In contrast, 4-(3′-chlorophenyl)-containing compound **18** displayed stronger topo I inhibitory activity but weaker topo II inhibitory activity. Similar results were observed in the case of 2-(4′-hydroxyphenyl)-containing compound (**J**) and respective chlorinated derivatives **17**, **20** and **23**. However, Compound **I** having 2-(3′-hydroxyphenyl) moiety displayed better relative potency for topo II than respective chlorinated analogs **16**, **19** and **22** while compounds **19** and **20** exhibited slightly stronger relative potency for topo I than compound **I**. The

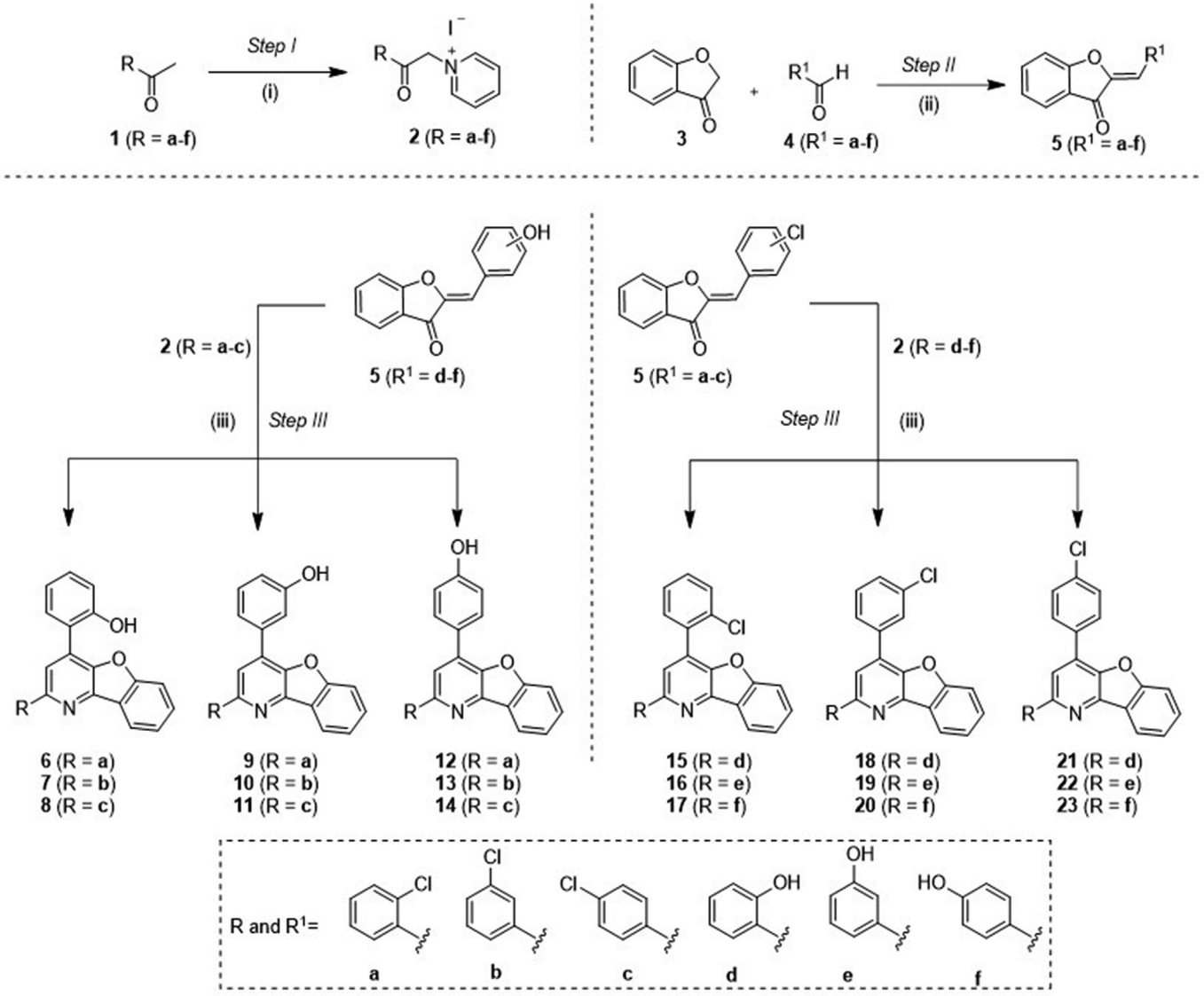


**Scheme 1.** General synthetic method of 2,4-chloro- and hydroxy-substituted diphenyl benzofuro[3,2-*b*]pyridines **6**–**23**; Reagents and conditions: i) iodine (1.0 equiv.), pyridine, 3 h, 140 °C, 52.2–93.0% yield; ii) $Al_2O_3$, $CH_2Cl_2$, 3 h, rt, 51.0–81.6% yield; iii) $NH_4OAc$ (10.0 equiv.), glacial acetic acid, 12–24 h, 100 °C, 8.9–36.5% yield.

topo inhibitory activity and antiproliferative activity would be affected by position of hydroxyl and chloride groups. Compounds **6**–**14** possessing hydroxyl group at 4-phenyl ring displayed significant dual topo I and II inhibitory activity, and strong antiproliferative activity. On the other hand, compounds **15**–**23** possessing hydroxyl group at 2-phenyl group showed comparatively low topo I and II inhibitory activity and/or antiproliferative activity. These results indicate the crucial role of hydroxyl group at 4-phenyl ring for displaying dual topo I and II inhibitory activity as well as antiproliferative activity. Generally, we observed positive correlation between dual topo I and II inhibitory activity and antiproliferative activity. Compounds bearing phenol on 4-position of central pyridine ring showed stronger antiproliferative activity than those of bearing phenol on 2-position (Fig. 5). In addition, dual topo I and II inhibitory activity and antiproliferative activity was not depending on the position of chlorophenyl on 2-position of central pyridine ring.

### 2.5. Mode of action of compound 14

Compound **14** showing the most potent dual topo I and II inhibitory activity was chosen for further analysis to determine its mode of action. Moreover, compound **14** inhibited most potently HCT15 cell growth (Table 1). Therefore, cell-based experiments to clarify the mode of action of compound **14** were performed with HCT15 cells.

#### 2.5.1. Compound *14* acted as a catalytic topo I and II dual inhibitor not a topo poison

Cleavable complex assay was first performed to assess whether compound **14** generated a truncated linear DNA which could be a surrogate marker for a topo poison. Since the topo poison like etoposide has ability to stabilize the transiently formed topo II-DNA cleavable complex leading to prevention of the transiently cleaved DNA double strand from being religated and consequently induction of undesirable short DNA [35]. As shown in Fig. 6A, etoposide made the truncated linear DNA while compound **14** did not. Kinetoplast DNA (kDNA) decatenation assay is a method to specifically evaluate the topo II inhibitory activity [36]. In order to confirm the topo II inhibitory activity of compound 14, we performed the assay with compound **14** using kDNA as a substrate. kDNA is a catenated network of thousands of interlocked closed

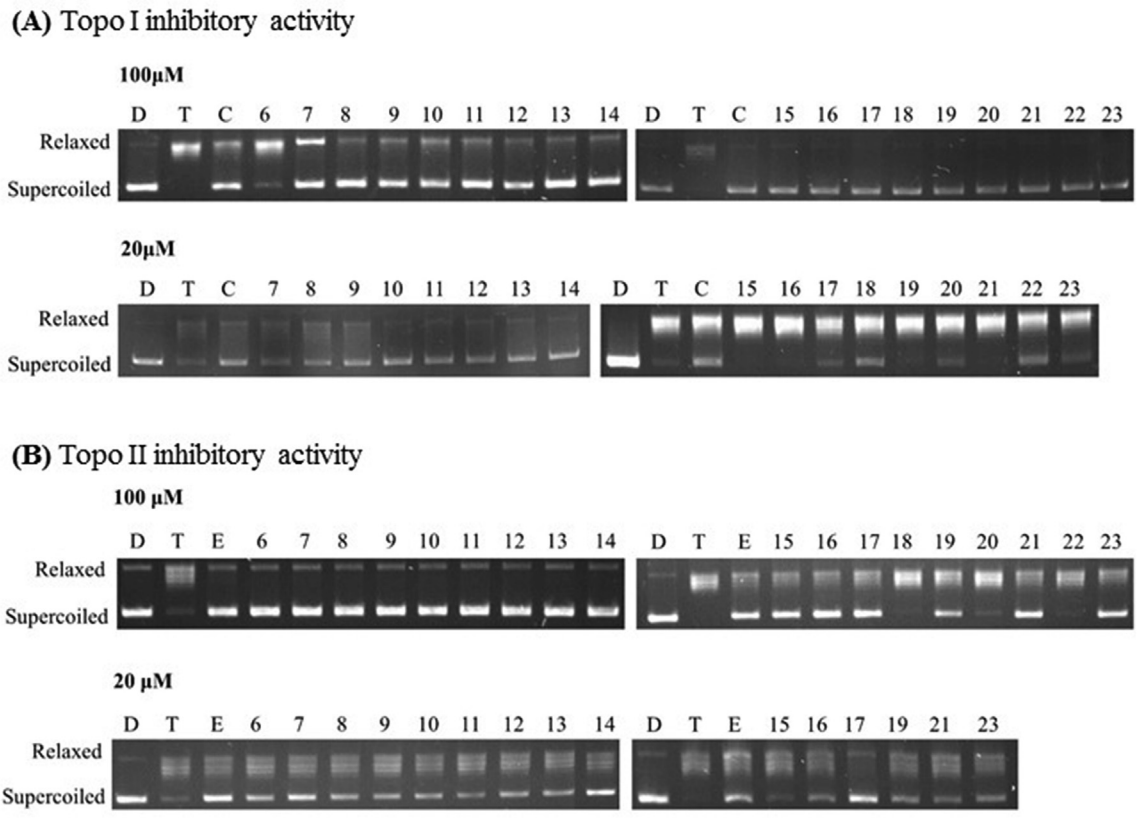


**Fig. 4.** DNA topo I (A) and topo II (B) inhibitory activity of the prepared compounds **6**–**23** at the concentrations of 100 μM and 20 μM. (A) Lane D: pBR322 only, Lane T: pBR322 + Topo I, Lane C: pBR322 + Topo I + Camptothecin, Lane 6–23: pBR322 + Topo I + compounds **6**–**23** at 100 μM or 20 μM. (B) Lane D: pBR322 only, Lane T: pBR322 + Topo II, Lane E: pBR322 + Topo II + Etoposide, Lane 6–23: pBR322 + Topo II + compounds **6**–**23** at 100 μM or 20 μM.

**Table 1**
Topo I and II inhibitory and antiproliferative activity of the prepared compounds **6**–**23**.

| Compounds | %Inhibition | | | | $IC_{50}$ (μM) | | |
|---|---|---|---|---|---|---|---|
| | Topo II | | Topo I | | HCT15 | T47D | HeLa |
| | 100 μM | 20 μM | 100 μM | 20 μM | | | |
| **Camptothecin** | | | 59.0[a]/55.8[b] | 34.1[a]/22[b] | 0.6 ± 0.02 | 2.1 ± 0.001 | 0.09 ± 0.01 |
| **Etoposide** | 86.9[a]/56.3[b] | 34.2[a]/30[b] | | | 5.4 ± 0.5 | 7.0 ± 0.05 | 9.1 ± 0.2 |
| **Adriamycin** | | | | | 1.0 ± 0.02 | 0.3 ± 0.02 | 1.2 ± 0.01 |
| **6** | 85.6 | 21.2 | 11.2 | NT | 0.4 ± 0.02 | 3.9 ± 0.2 | 2.8 ± 0.1 |
| **7** | 84.0 | 31.2 | 59.8 | 13.0 | 0.01 ± 0.001 | 0.4 ± 0.04 | 5.2 ± 0.4 |
| **8** | 86.7 | 21.6 | 82.1 | 31.7 | >50 | >50 | 9.5 ± 0.1 |
| **9** | 82.9 | 14.4 | 71.8 | 33.4 | 1.6 ± 0.2 | 1.5 ± 0.1 | 4.4 ± 0.04 |
| **10** | 85.4 | 22.1 | 66.3 | 69.0 | 0.4 ± 0.01 | 1.4 ± 0.01 | 4.3 ± 0.1 |
| **11** | 87.9 | 9.3 | 78.1 | 71.3 | 0.2 ± 0.02 | 2.1 ± 0.03 | 5.7 ± 0.03 |
| **12** | 92.8 | 19.1 | 82.2 | 67.8 | 0.4 ± 0.02 | 6.1 ± 0.06 | 3.9 ± 0.01 |
| **13** | 95.4 | 23.1 | 92.1 | 44.1 | 0.2 ± 0.01 | 1.9 ± 0.001 | 0.9 ± 0.001 |
| **14** | 100 | 59.8 | 95.6 | 47.9 | 0.2 ± 0.03 | 5.9 ± 0.1 | 4.3 ± 0.2 |
| **15** | 58.2 | 20.7 | 41.7 | 0 | 0.3 ± 0.02 | 3.0 ± 0.1 | 10.9 ± 0.3 |
| **16** | 60.2 | 17.2 | 42.7 | 0.6 | 1.4 ± 0.03 | 0.1 ± 0.02 | 4.3 ± 0.03 |
| **17** | 52.7 | 47.8 | 63.5 | 10.0 | 46.2 ± 0.8 | 0.8 ± 0.1 | 15.9 ± 0.1 |
| **18** | 4.7 | NT | 79.6 | 14.4 | >50 | >50 | >50 |
| **19** | 35.0 | 6.2 | 83.8 | 0 | 5.9 ± 0.01 | 1.2 ± 0.03 | 6.4 ± 0.04 |
| **20** | 4.9 | NT | 76.6 | 3.2 | 5.9 ± 0.01 | >50 | >50 |
| **21** | 55.8 | 4.7 | 64.5 | 0 | >50 | >50 | >50 |
| **22** | N/A | NT | 69.5 | 15.1 | >50 | 2.0 ± 0.01 | 11.1 ± 0.04 |
| **23** | 65.6 | 28.4 | 87.5 | 0 | 21.3 ± 0.9 | 11.6 ± 0.1 | 11.8 ± 0.4 |

Each data represents mean ± S.D. from three different experiments performed in triplicate.
NT: Not tested, NA; not active, [a] value for compounds **6**–**14**; [b] value for compounds **15**–**23.**
HCT15: human colorectal adenocarcinoma cell line; T47D: human breast cancer cell line; HeLa: human cervix tumor cell line.
Camptothecin: positive control for topo I and cytotoxicity; Etoposide: positive control for topo II and cytotoxicity; Adriamycin: positive control for cytotoxicity.

circular DNA. Ellipticin and etoposide were used as positive controls. The inhibitory activity of compound **14** was not as effective as positive controls. However, its suppressive effect on topo IIα showed nice concentration dependency as shown in Fig. 6B. This

**Table 2**
Relative topo I and II inhibitory potencies of representative compounds compared to etoposide or camptothecin.

| Relative potency[a] for % inhibition compared to positive control (Topo II: Etoposide and Topo I: Camptothecin) | | | | | | | | | |
|---|---|---|---|---|---|---|---|---|---|
| Compounds | Topo II | | Topo I | | Compounds | Topo II | | Topo I | |
| | 100 μM | 20 μM | 100 μM | 20 μM | | 100 μM | 20 μM | 100 μM | 20 μM |
| **A** | 0.08 | NT | NA | NT | **10** | 0.98 | 0.65 | 1.12 | 2.02 |
| **B** | 0.05 | NT | 0.1 | NT | **11** | 1.01 | 0.27 | 1.32 | 2.09 |
| **C** | 0.10 | NT | 0.26 | NT | **12** | 1.07 | 0.56 | 1.39 | 1.99 |
| **D** | 0.03 | NT | 0.01 | NT | **13** | 1.10 | 0.77 | 1.56 | 1.29 |
| **E** | 0.04 | NT | NA | NT | **14** | 1.15 | 1.75 | 1.62 | 1.40 |
| **F** | 0.04 | NT | 0.02 | NT | **15** | 1.03 | 0.69 | 0.75 | NA |
| **G** | 0.08 | NA | 0.02 | NT | **16** | 1.07 | 0.57 | 0.77 | 0.03 |
| **H** | 0.66 | 0.05 | 0.63 | NA | **17** | 0.94 | 1.59 | 1.14 | 0.45 |
| **I** | 1.30 | 1.77 | 1.19 | 0.05 | **18** | 0.08 | NT | 1.43 | 0.65 |
| **J** | 1.02 | 0.90 | 0.50 | NT | **19** | 0.62 | 0.21 | 1.50 | NA |
| **6** | 0.98 | 0.62 | 0.18 | NT | **20** | 0.09 | NT | 1.37 | 0.15 |
| **7** | 0.97 | 0.91 | 1.01 | 0.38 | **21** | 0.99 | 0.16 | 1.16 | NA |
| **8** | 0.99 | 0.63 | 1.39 | 0.93 | **22** | NA | NT | 1.25 | 0.69 |
| **9** | 0.95 | 0.42 | 1.22 | 0.98 | **23** | 1.17 | 0.95 | 1.57 | NA |

[a] Relative potency: % inhibition of compound/% inhibition of positive control, NT: not tested, NA: not active.

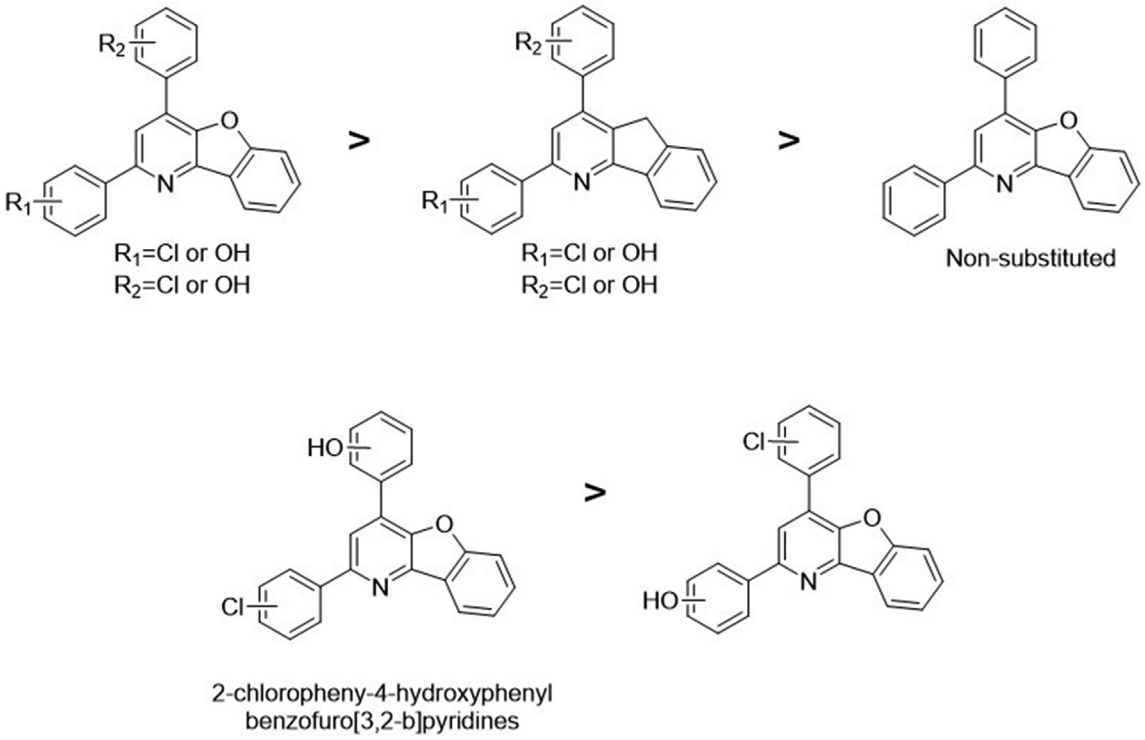


**Fig. 5.** Structure-activity relationship study of 2,4-chloro- and hydroxy-substituted diphenyl benzofuro[3,2-*b*]pyridines.

implies that the compound **14** indisputably holds considerable topo IIα inhibitory activity. Band depletion assay was accomplished to confirm that compound **14** did not induce topo II-DNA complex in cancer cells. After compound **14** and etoposide were treated at concentration of 50 μM, respectively, with HCT15 cells for 2 h, and then cell lysates were electrophoresed and western blotted to check the remained free topo II. The topo II-DNA covalent complex induced by etoposide was depleted during DNA precipitation process as described in method. As shown in Fig. 6C, free topo II was not detected in etoposide-treated HCT15 cell lysate but it was detected in compound **14**-treated one. Comet assay was further utilized to determine the DNA damage caused by compound **14**, etoposide and ICRF-187. The extent of comet (tail) formation indicates the DNA strand breaks. Fig. 6D indicates that compound **14** (6.3 ± 1.3% at 30 μM) almost did not induce tail compared to untreated control (3.0 ± 1.1%) like ICRF-187 (5.5 ± 1.9% at 30 μM), well-known topo II catalytic inhibitor [37], while etoposide, a well-known topo II poison, induced a significant DNA damage (the percent of tail DNA induced by etoposide: 46.3 ± 9.2% at 10 μM and 65.5 ± 9.8% at 30 μM) as expected. When DNA was damaged such as DNA double strand break induced by etoposide in mammalian cells, histones are phosphorylated and become γ-H2AX. γ-H2AX is widely used as a marker for DNA damage [38]. After 30 μM treatment of each of etoposide, ICRF-187 and compound 14, the changes on γ-H2AX expression was analyzed by western blotting. As shown in Fig. 6E, the significant increase of γ-H2AX protein level in

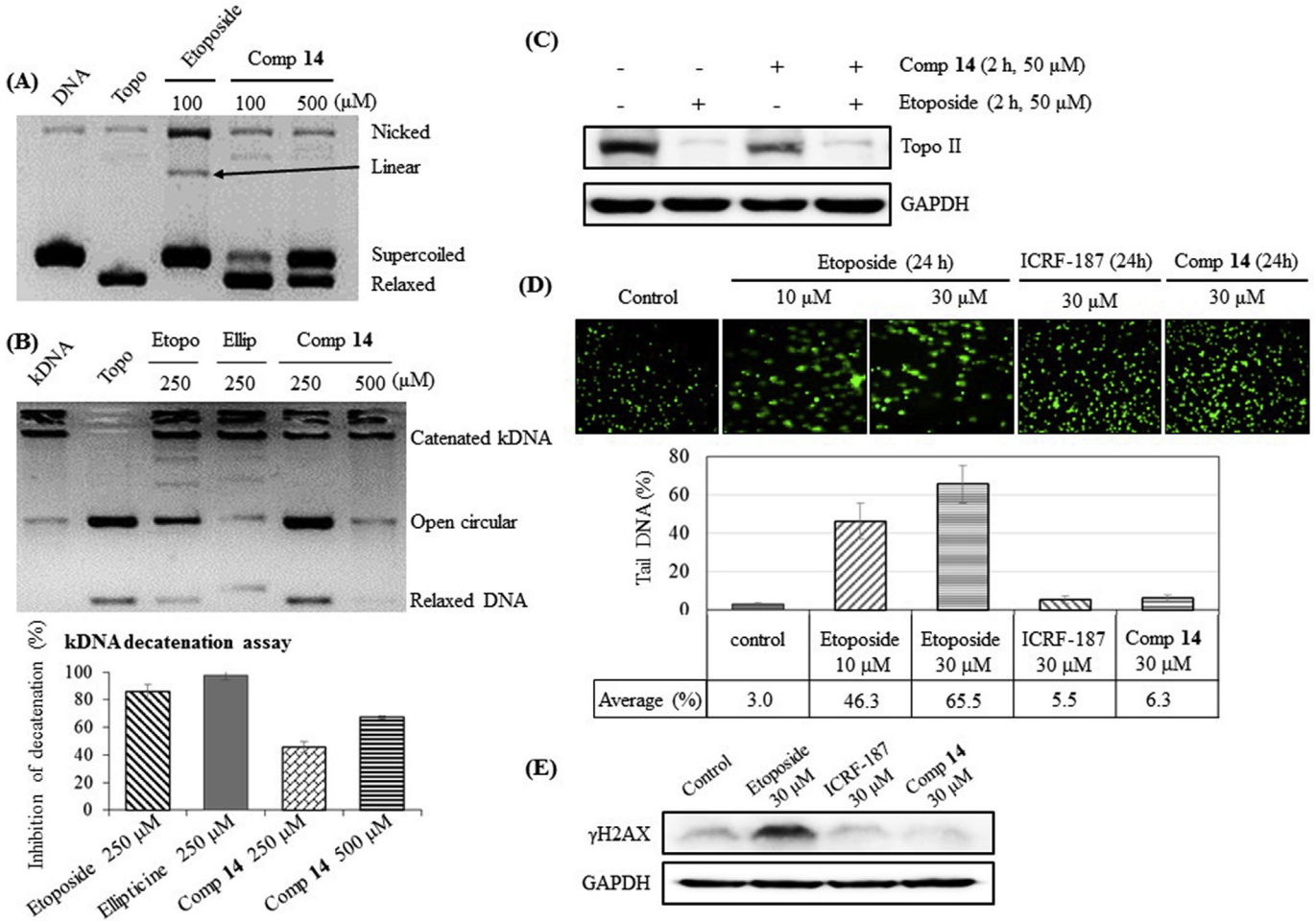


**Fig. 6.** (A) Cleavable complex assay: To determine whether topo II poison or catalytic inhibitor, 250 ng of pBR322 DNA was treated with 3 units of topo II for 10 min prior to treatment of etoposide (100 μM) or compound **14** (100 μM and 500 μM). After incubation for additional 30 min at 37 °C, the agarose gel electrophoresis was performed. A linear band on the gel for compound **14** was not observed reflecting that it worked as a catalytic inhibitor. (B) kDNA decatenation assay: The assay was performed in a total reaction volume of 10 μL containing 75 ng of kDNA, each of compounds in final concentration of 250 or 500 μM and 3 units of top II. The reaction mixture was incubated for 30 min at 37 °C and then terminated by the addition of 2.5 μL of stop solution (5% SDS, 25% ficoll and 0.05% bromphenol blue) followed by treatment with 0.25 mg/ml proteinase K at 37 °C for 30 min. Samples were resolved by electrophoresis on a 1.2% (w/v) agarose gel containing 0.5 μg/mL ethidium bromide in TAE buffer (*upper* panel). The quantification of product formed in the *upper* panel was graphed in *lower* panel. (C) Band depletion assay: Whether functioning as a topo poison or a catalytic inhibitor can be defined by looking at free topo II band. The topo II covalently bound to DNA was depleted during DNA precipitation process after treatment of topo II poison like etoposide. The cells seeded in a density of $2 \times 10^5$ were treated with each of etoposide and compound **14** for 2 h at 37 °C and then were harvested and lysed by denaturing agent of 62.5 mM Tris-HCl (pH 6.8) containing 1 mM EDTA and 2% SDS. The prepared lysates were detected by Western blotting. (D) Comet assay: To evaluate whether compound **14** induced DNA damage like a topo poison, etoposide, each of compound **14**, etoposide and ICRF-187 was treated with HCT15 cells for 24 h in final concentrations of 10 or 30 μM. Then harvested cells were executed for alkaline unwinding process and electrophoresis under the alkaline condition followed by staining with SYBR Green. The percent DNA in tail was analyzed by Komet 5.0 software. Data were represented both by imaging (*upper* panel) and vertical bar graph (*lower* panel) by randomly selecting comet lengths of HCT15 cells. Etoposide generated tail significantly at both concentration of 10 and 30 μM while ICRF-187 and compound **14** almost did not at 30 μM. (E) The effect of compounds on the expression level of γ-H2AX: each of compounds, etoposide, ICRF-187 and compound **14**, was treated with HCT15 cells in concentrations of 30 μM for 24 h followed by lysis. 60 μg of protein per sample was resolved by 12% SDS-PAGE and then analyzed by western blot. (For interpretation of the references to colour in this figure legend, the reader is referred to the web version of this article.)

compared to the untreated control was detected in etoposide-treated HCT15 cells while not observed in ICRF-187- and compound **14**-treated cells. This result is consistent with the degree of comet formation (Fig. 6D). Based on results of cleavable complex assay and band depletion assay, it could be concluded that the compound **14** did not act as topo poison unlike etoposide, in contrast compound **14** functioned as topo II catalytic inhibitor. In addition, since compound **14** inhibited both topo I and II with almost no generation of tail in comet assay, compound **14** can be reasonably ratiocinated as a catalytic topo I and II dual inhibitor.

### 2.5.2. Compound **14** did not intercalate into DNA

To check whether compound **14** intercalate into DNA, ethidium bromide (EtBr) displacement assay was performed with calf thymus DNA (ctDNA) intercalated with EtBr by increasing concentration of compound **14** and amsacrine (m-AMSA), well-known DNA intercalative topo II poison [8]. The fluorescence of EtBr was decreased by addition of m-AMSA in dose-dependent manner (Fig. 7A) because m-AMSA displaced EtBr through intercalation into DNA. The released EtBr from ctDNA lost fluorescence due to its free rotation in the solution. The addition of compound **14** did not reduce the fluorescence intensity of EtBr (Fig. 7B) reflecting that compound **14** could not intercalate into DNA. Taken together compound **14** is non-intercalative catalytic topo I and II dual inhibitor.

### 2.5.3. Compound **14** induced apoptosis in HCT15 cells

Topo plays important roles in fast tumor cell proliferation rate [1,2], therefore inhibition of endogenous topo I and II as well as

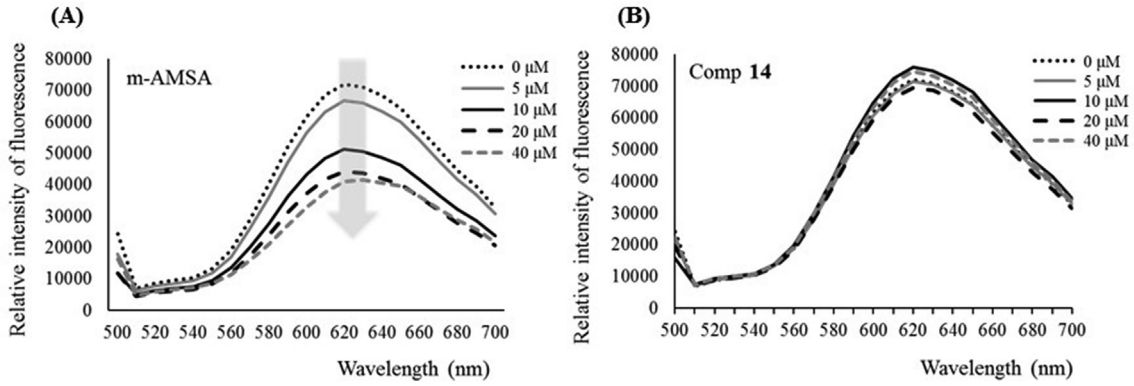


**Fig. 7.** Competitive EtBr displacement assay: The mixture of ctDNA (30 μM) and EtBr (20 μM) in the 10 mM tris buffer solution (pH 7.2) was incubated for 30 min at room temperature followed by addition of m-AMSA (A) and compound **14** (B) at the designated concentrations with continuous incubation for additional 30 min. The fluorescence intensity of each well was measured with excitation at 471 nm. The emission spectrum was collected at 500–700 nm. Addition of m-AMSA, well known DNA intercalative topo II poison, decreased EtBr-induced fluorescence in dose-dependent manner but compound **14** did not.

apoptosis induction of cancer cells might be efficient strategy for development of anticancer agent [39]. To evaluate the effect of compound **14** on endogenous topo I and II, HCT15 cells were pre-treated for 24 h with camptothecin, etoposide and compound **14** followed by preparation of nuclear fraction of each compound-treated cells. Camptothecin and etoposide were used as positive controls as topo I and topo II inhibitors, respectively. The effect of compound **14** was relatively insignificant than the positive controls in cells (Fig. 8A and B). We assume that this phenomenon is due to the poor solubility of compound **14**, which made it difficult to penetrate through the cell membranes. However, it still showed inhibitory activity in a concentration dependent manner against both topo I and topo II in the cellular system. Thus, compound **14** is a valid candidate as a dual inhibitor of topo I and topo II. It has been proposed that a ratio of Bax (an apoptosis promoter) to Bcl-2 (an apoptosis inhibitor) rules apoptosis in various types of cancer cells as the response to chemotherapy; chemotherapeutic drugs induce an increase of Bax and decrease of Bcl-2 leading to apoptosis and cell death [40,41]. The upregulated ratio of Bax to Bcl-2 activates caspase which consequently makes poly (ADP-ribose) polymerase (PARP) to be cleaved. Cleavage of PARP by caspase is reflected as a feature of apoptosis [42]. Compound **14** was evaluated for its ability to induce apoptosis of HCT15 cells. Compound **14** treatment increased apoptotic proteins such as cleaved PARP and Bax and simultaneously decreased anti-apoptotic protein, Bcl-2 in HCT15 cells in dose-dependent manner (Fig. 8C).

## 3. Conclusion

Total eighteen 2,4-chloro- and hydroxy-substituted diphenyl benzofuro[3,2-*b*]pyridines were designed and synthesized systematically and evaluated for their topo I and II inhibitory activity, and antiproliferative activity against several human cancer cell lines. Synthesized compounds were found to be more anti-proliferative to HCT15 cancer cell line. Most of the tested compounds displayed dual topo I and topo II inhibitory activity. SAR study revealed that the introduction of novel benzofuropyridine moiety significantly enhanced the topo I and II inhibitory activity as well as antiproliferative activity as compared to corresponding indenopyridine derivatives. Introduction of hydroxyphenyl moiety at 4-position of central pyridine ring would be crucial to exhibit dual topo I and II inhibitory activity as well as antiproliferative activity. Compound **14** was selected to study the mode of action since it showed the most potent dual topo I and II inhibition and antiproliferative activity in HCT15 cell. Compound **14** functioned as potent non-intercalative catalytic topo I and II dual inhibitor and induced apoptosis in HCT15 cell through increase of Bax, decrease of Bcl-2 and increase of PARP cleavage. This study might provide valuable information for the researchers working on benzofuran derivatives and topoisomerase as potential anticancer drug target.

## 4. Experimental

Commercially available starting materials and reagents were purchased from Sigma-Aldrich, TCI Chemicals, Alfa-Aesar, and Junsei, and were used without further purification. HPLC grade acetonitrile (ACN) and methanol were purchased from Burdick and Jackson, USA. Column chromatography was carried out using silica gel (Kieselgel 60, 230–400 mesh, Merck). Thin layer chromatography (TLC) was performed on silica gel plates (Kieselgel 60 $F_{254}$, Merck) having layer thickness of 0.25 mm. Melting points were recorded using open capillary tube on electrothermal 1A 9100 digital melting point apparatus and were uncorrected. $^{1}$H NMR (250 MHz) and $^{13}$C NMR (62.5 MHz) spectra were recorded in Bruker AMX 250 (250 MHz, FT) spectrometer using $CDCl_3$ and DMSO-$d_6$ as solvent, and tetramethylsilane (TMS) as internal standard. All the chemical shifts values ($\delta$) were recorded in parts per million (ppm) and coupling constants ($J$) in hertz (Hz).

HPLC analyses were performed using two Shimadzu LC-10AT pumps gradient-controlled HPLC system equipped with Shimadzu system controller (SCL-10A VP) and photo diode array detector (SPD-M10A VP) utilizing Shimadzu LC Solution program. Sample volume of 10 μL, was run in Waters X- Terra® 5 μM reverse-phase $C_{18}$ column (4.6 × 250 mm) with a gradient elution of 85%–100% of B in A for 10 min followed by 100%–85% of B in A for 10 min at a flow rate of 0.7 mL/min at 254 nm UV detection, where mobile phase A was doubly distilled water with 50 mM ammonium formate (AF) and B was 100% ACN. Purity of compound is stated as percent (%) and retention time in minutes.

Mass spectra of the compound were recorded with Advion Expression CMS® ESI-MS spectrometry (Advion, Ithaca, NY, USA), using methanol: water: formic acid (80: 20: 0.1) as a mobile phase.

### 4.1. General method for preparation of 2 (R = a-f)

Pyridinium iodide salts **2** (R = **a-f**) were synthesized by reacting aryl methyl ketones **1** (R = **a-f**) with equivalent amount of iodine in pyridine at 140 °C for 3 h at reflux condition. The reaction mixture was cooled to room temperature which resulted precipitation. Precipitate formed was filtered and washed with cold pyridine

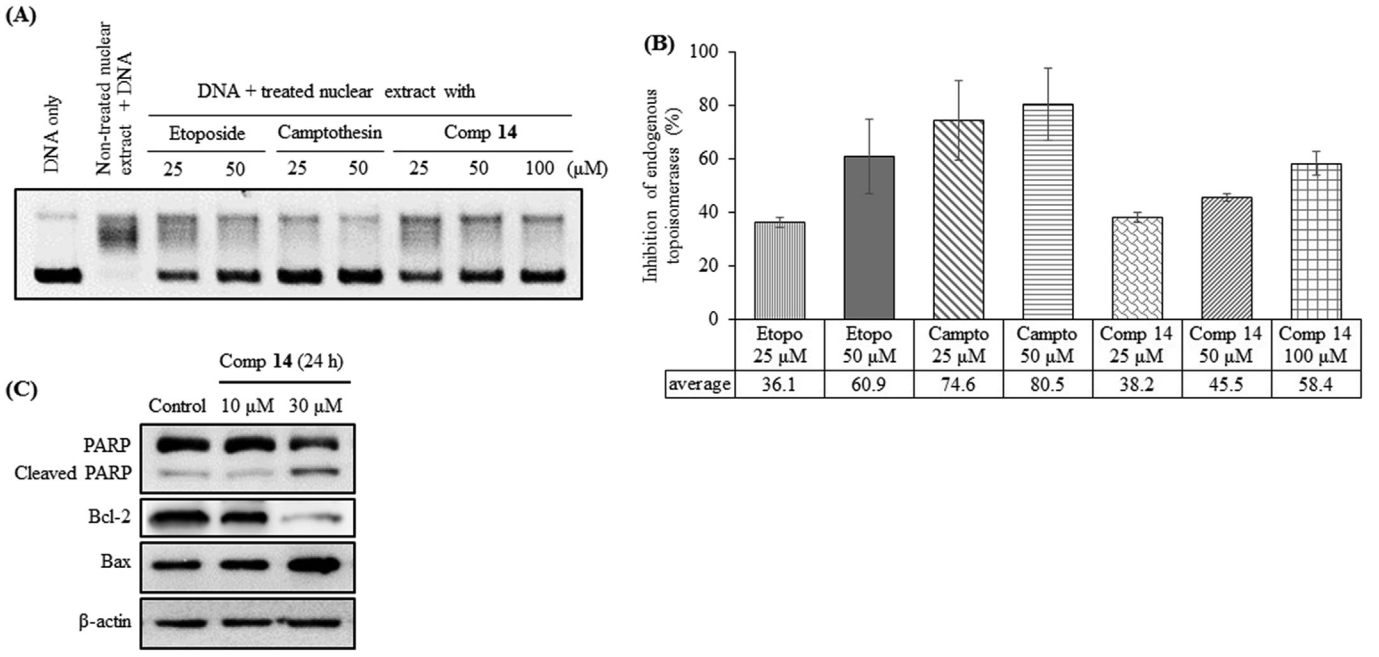


**Fig. 8.** (A) Endogenous topo inhibition assay: Nuclear lysates of HCT15 cells, prepared after treatment with etoposide, camptothecin and compound **14** in concentrations of 25, 50 or 100 μM for 24 h, were incubated for 30 min with 100 ng pBR322 plasmid at 37 °C to evaluate the inhibitory activity of each compound against endogenous topo I and II. DNA band visualized by transillumination with UV light (A) is a representative image, obtained from three different experiments. (B) The average inhibition percent of each compound was quantified and plotted from three experiments. (C)The effect of compound **14** on apoptotic proteins: After compound **14** was treated with HCT15 cells in concentrations of 10 and 30 μM for 24 h, cells were harvested and lysed. The supernatants of compound **14**-treated cell lysates after lysis were electrophoresed on 12% SDS-PAGE gels. Western blotting analyses were then performed in according to the method described in the experimental. Cleaved PARP, Bcl-2, and Bax were detected in compound **14**-treated HCT15 cells.

followed by drying overnight to yield 52.2–93.0% of **2** (R = **a-f**). Compounds were used without further purification.

### 4.2. General method for preparation of 5 ($R^1$ = a-f)

To the mixture of benzofuran-3(*2H*)-one (**3**) and aryl aldehydes (1.5 equivalent) **4** ($R^1$ = **a-f**) in methylene chloride was added aluminum oxide and the reaction mixture was stirred at 25 °C for 3 h. The mixture was then filtered and washed with ethyl acetate. Silica gel column chromatography was used to purify the compounds. Total six benzofuran-3(*2H*)-one intermediates **5** ($R^1$ = **a-f**) were synthesized at the yield of 51.0–81.6%.

#### 4.2.1. Synthesis of 2-(2-chlorobenzylidene)benzofuran-3(2H)-one (*5a*)

The procedure described in Section 4.2 was employed with benzofuran-3(*2H*)-one (1.34 g, 10.0 mmol) and 2-chlorobenzahdehyde (1.69 mL, 15.0 mmol) to yield 2.02 g (78.5%) as a yellow solid.

TLC (ethyl acetate/*n*-hexane = 1:4 v/v) $R_f$ = 0.28; Mp: 144.6–145.1 °C

**$^1$H NMR** (250 MHz, $CDCl_3$) δ 8.33 (dd, *J* = 7.7, 1.82 Hz, 1H, benzofuro H-4), 7.79 (d, *J* = 7.64 Hz, 1H, benzofuro H-7), 7.64 (td, *J* = 7.22, 1.42 Hz, 1H, benzofuro H-6), 7.46–7.18 (m, 6H, benzofuro H-5, 2-phenyl H-3, H-4, H-5, H-6 and = C**H**-).

**$^{13}$C NMR** (62.5 MHz, $CDCl_3$) δ 184.75, 166.40, 147.82, 137.28, 136.16, 132.46, 130.81, 130.62, 130.23, 127.26, 125.06, 123.91, 121.72, 113.14, 108.21.

#### 4.2.2. Synthesis of 2-(3-chlorobenzylidene)benzofuran-3(2H)-one (*5b*)

The procedure described in Section 4.2 was employed with benzofuran-3(*2H*)-one (1.34 g, 10.0 mmol) and 3-chlorobenzahdehyde (1.70 mL, 15.0 mmol) to yield 2.14 g (81.6%) as a yellow solid.

TLC (ethyl acetate/*n*-hexane = 1:4 v/v) $R_f$ = 0.27; Mp: 136.2–136.7 °C

**$^1$H NMR** (250 MHz, DMSO-$d_6$) δ 8.01–7.93 (m, 2H, benzofuro H-4 and H-6), 7.83–7.77 (m, 2H, 2-phenyl H-4 and H-6), 7.59–7.50 (m, 3H, benzofuro H-7, 2-phenyl H-2 and H-5), 7.32 (t, *J* = 7.35 Hz, 1H, benzofuro H-5), 6.93 (s, 1H, =C**H**-).

**$^{13}$C NMR** (62.5 MHz, DMSO-$d_6$) δ 183.61, 165.42, 146.41, 137.25, 135.06, 133.16, 130.01, 129.92, 129.20, 125.26, 124.56, 120.98, 121.72, 113.43, 111.01.

#### 4.2.3. Synthesis of 2-(4-chlorobenzylidene)benzofuran-3(2H)-one (*5c*)

The procedure described in Section 4.2 was employed with benzofuran-3(*2H*)-one (1.34 g, 10.0 mmol) and 4-chlorobenzahdehyde (2.11 mL, 15.0 mmol) to yield 1.48 g (57.7%) as a yellow solid.

TLC (ethyl acetate/*n*-hexane = 1:4 v/v) $R_f$ = 0.25; Mp: 180.7–181.2 °C

**$^1$H NMR** (250 MHz, DMSO-$d_6$) δ 8.01 (d, *J* = 8.55 Hz, 2H, 2-phenyl H-2 and H-6), 7.79 (d, *J* = 7.45 Hz, 2H, 2-phenyl H-3 and H-5), 7.59–7.54 (m, 3H, benzofuro H-4, H-6 and H-7), 7.32 (t, *J* = 7.5 Hz, 1H, benzofuro H-5), 6.96 (s, 1H, =C**H**-).

**$^{13}$C NMR** (62.5 MHz, DMSO-$d_6$) δ 183.74, 165.54, 146.58, 137.96, 134.76, 133.03 (2C), 130.94, 129.24 (2C), 124.48, 124.23, 120.83, 113.34, 110.92).

#### 4.2.4. Synthesis of 2-(2-hydroxybenzylidene)benzofuran-3(2H)-one (*5d*)

The procedure described in Section 4.2 was employed with benzofuran-3(*2H*)-one (0.80 g, 6.0 mmol) and salicylaldehyde (0.96 mL, 9.0 mmol) to yield 0.98 g (69.9%) as a yellow solid.

TLC (ethyl acetate/*n*-hexane = 1:2 v/v) $R_f$ = 0.29; Mp: 248.2–248.7 °C

**$^1$H NMR** (250 MHz, DMSO-$d_6$) δ 10.43 (s, 1H, 2-phenyl 2-OH), 8.15 (d, $J$ = 7.02 Hz, 1H, 2-phenyl H-6), 7.80–7.76 (m, 2H, benzofuro H-4 and H-6), 7.55 (d, $J$ = 8.7 Hz, 1H, benzofuro H-7), 7.34–7.24 (m, 3H, benzofuro H-5, 2-phenyl H-5 and = C**H**-), 6.97–6.93 (m, 2H, 2-phenyl H-3 and H-4).

**$^{13}$C NMR** (62.5 MHz, DMSO-$d_6$) δ 183.41, 165.24, 157.51, 145.82, 137.37, 131.89, 131.15, 124.17, 123.81, 121.03, 119.68, 118.67, 115.82, 113.19, 106.55.

#### 4.2.5. Synthesis of 2-(3-hydroxybenzylidene)benzofuran-3(2H)-one (**5e**)

The procedure described in Section 4.2 was employed with benzofuran-3(*2H*)-one (1.34 g, 10.0 mmol) and 3-hydroxybenzahdehyde (1.83 g, 15.0 mmol) to yield 1.26 g (51.0%) as a yellow solid.

TLC (ethyl acetate/*n*-hexane = 1:2 v/v) $R_f$ = 0.24; Mp: 275.8–276.3 °C

**$^1$H NMR** (250 MHz, DMSO-$d_6$) δ 9.75 (s, 1H, 2-phenyl 3-OH), 7.83–7.77 (m, 2H, benzofuro H-4 and H-6), 7.59 (d, $J$ = 8.35 Hz, 1H, benzofuro H-7), 7.43–7.26 (m, 4H, benzofuro H-5, 2-phenyl H-2, H-5 and H-6), 6.89–6.84 (m, 2H, 2-phenyl H-4 and = C**H**-).

**$^{13}$C NMR** (62.5 MHz, DMSO-$d_6$) δ 183.76, 165.50, 157.69, 156.27, 137.82, 133.0, 130.09, 124.42, 124.08, 122.81, 120.94, 117.67, 117.62, 113.24, 112.65.

#### 4.2.6. Synthesis of 2-(4-hydroxybenzylidene)benzofuran-3(2H)-one (**5f**)

The procedure described in Section 4.2 was employed with benzofuran-3(*2H*)-one (0.80 g, 6.0 mmol) and 4-hydroxybenzahdehyde (1.10 g, 9.0 mmol) to yield 1.06 g (74.1%) as a yellow solid.

TLC (ethyl acetate/*n*-hexane = 1:2 v/v) $R_f$ = 0.27; Mp: 204.9–205.6 °C

**$^1$H NMR** (250 MHz, DMSO-$d_6$) δ 10.26 (br s, 1H, 2-phenyl 4-OH), 7.86 (d, $J$ = 8.76 Hz, 2H, 2-phenyl H-2 and H-6), 7.79–7.73 (m, 2H, benzofuro H-4 and H-6), 7.52 (d, $J$ = 7.37 Hz, 1H, benzofuro H-7), 7.28 (t, $J$ = 7.37 Hz, 1H, benzofuro H-5), 6.91–6.88 (m, 3H, 2-phenyl H-3 and H-5 and = C**H**-).

**$^{13}$C NMR** (62.5 MHz, DMSO-$d_6$) δ 183.72, 165.20, 159.98, 144.90, 137.36, 133.95 (2C), 124.29, 123.95, 123.03, 121.53, 116.38 (2C), 113.64, 113.35.

### 4.3. General method for preparation of 6–23

Based upon the modified Kröhnke pyridine synthesis, 2,4-chloro- and hydroxy-substituted diphenyl benzofuro[3,2-*b*]pyridines (**6**–**23**) were synthesized. To the mixture of benzofuran-3(*2H*)-one intermediates **5** ($R^1$ = **a-f**) and aryl pyridinium iodide salts **2** (R = **a-f**) in glacial acetic acid, was added anhydrous ammonium acetate (10.0 equiv.). The mixture was stirred at 100 °C for 12–24 h. The mixture was then extracted with ethyl acetate, washed with water and brine. The anhydrous magnesium sulfate was used to dry the organic layer and filtered. For the purification, silica gel column chromatography was utilized with the gradient elution of ethyl acetate and *n*-hexane to afford solid compounds **6**–**23** in 8.9–36.5% yield.

#### 4.3.1. Synthesis of 2-(2-(2-chlorophenyl)benzofuro[3,2-b]pyridin-4-yl)phenol (**6**)

The compound was synthesized as described in section 4.3 with **5d** (0.24 g, 1.0 mmol), dry ammonium acetate (0.77 g, 10.0 mmol), **2a** (0.36 g, 1.0 mmol) with glacial acetic acid (2 mL) to yield 66 mg (17.7%) of a yellow solid.

TLC (ethyl acetate/*n*-hexane = 2:5 v/v) $R_f$ = 0.28; Mp: 192.7–193.3 °C; HPLC: Retention time: 9.27 min, purity: 100.0%; ESI-MS: *m/z* calcd for $C_{23}H_{14}ClNO_2$ $[M+H]^+$: 372.08; found $[M+H]^+$: 372.98.

**$^1$H NMR** (250 MHz, $CDCl_3$) δ 8.31 (d, $J$ = 7.65 Hz, 1H, benzofuro H-4), 7.82 (s, 1H, pyridine H-3), 7.72–7.69 (m, 1H, benzofuro H-7), 7.62–7.28 (m, 8H, 2-phenyl H-3, H-4, H-5, H-6, 4-phenyl H-4, H-6, benzofuro H-5 and H-6), 7.09 (td, $J$ = 7.53, 1.13 Hz, 1H, 4-phenyl H-5), 7.01 (dd, $J$ = 8.15, 0.93 Hz, 1H, 4-phenyl H-3).

**$^{13}$C NMR** (62.5 MHz, $CDCl_3$) δ 157.72, 153.85, 153.33, 146.50, 144.59, 139.18, 132.69, 132.17, 131.39, 131.25, 130.29, 129.91, 129.71, 129.55, 127.33, 124.15, 124.09, 123.53, 122.00, 121.40, 121.20, 117.62, 112.49.

#### 4.3.2. Synthesis of 2-(2-(3-chlorophenyl)benzofuro[3,2-b]pyridin-4-yl)phenol (**7**)

The compound was synthesized as described in section 4.3 with **5d** (0.24 g, 1.0 mmol), dry ammonium acetate (0.77 g, 10.0 mmol), **2b** (0.36 g, 1.0 mmol) with glacial acetic acid (2 mL) to yield 70 mg (20.0%) of a yellow solid.

TLC (ethyl acetate/*n*-hexane = 2:5 v/v) $R_f$ = 0.32; Mp: 224.5–224.8 °C; HPLC: Retention time: 9.18 min, purity: 98.2%; ESI-MS: *m/z* calcd for $C_{23}H_{14}ClNO_2$ $[M+H]^+$: 372.08; found $[M+H]^+$: 372.19.

**$^1$H NMR** (250 MHz, DMSO-$d_6$) δ 9.97 (br S, 1H, 4-phenyl 2-OH) 8.29 (br, 2H, benzofuro H-4 and 2-phenyl H-2), 8.18 (br, 2H, pyridine H-3 and 2-phenyl H-6), 7.78 (d, $J$ = 8.27 Hz, 1H, benzofuro H-7), 7.69–7.49 (m, 5H, 2-phenyl H-4, H-5, 4-phenyl H-4, H-6 and benzofuro H-6), 7.36 (td, $J$ = 7.22, 1.55 Hz, 1H, benzofuro H-5), 7.08–6.98 (m, 2H, 4-phenyl H-3 and H-5).

**$^{13}$C NMR** (62.5 MHz, DMSO-$d_6$) δ 157.32, 155.28, 150.89, 147.11, 143.54, 141.14, 133.97, 131.61, 131.39, 130.90, 130.84, 129.93, 128.69, 126.70, 125.65, 124.14, 123.07, 121.27, 120.71, 120.52, 119.48, 116.34, 112.72.

#### 4.3.3. Synthesis of 2-(2-(4-chlorophenyl)benzofuro[3,2-b]pyridin-4-yl)phenol (**8**)

The compound was synthesized as described in section 4.3 with **5d** (0.24 g, 1.0 mmol), dry ammonium acetate (0.77 g, 10.0 mmol), **2c** (0.36 g, 1.0 mmol) with glacial acetic acid (2 mL) to yield 0.11 g (30.4%) of a white solid.

TLC (ethyl acetate/*n*-hexane = 2:5 v/v) $R_f$ = 0.32; Mp: 316.4–316.8 °C; HPLC: Retention time: 9.05 min, purity: 95.7%; ESI-MS: *m/z* calcd for $C_{23}H_{14}ClNO_2$ $[M+H]^+$: 372.08; found $[M+H]^+$: 372.13.

**$^1$H NMR** (250 MHz, DMSO-$d_6$) δ 10.02 (br S, 1H, 4-phenyl 2-OH) 8.27–8.22 (m, 3H, benzofuro H-4, 2-phenyl H-2 and H-6), 8.13 (s, 1H, pyridine H-3), 7.77 (d, $J$ = 8.15 Hz, 1H, benzofuro H-7), 7.68–7.48 (m, 5H, 2-phenyl H-3, H-5, 4-phenyl H-4, H-6 and benzofuro H-6), 7.36 (td, $J$ = 7.50, 1.55 Hz, 1H, benzofuro H-5), 7.07–6.97 (m, 2H, 4-phenyl H-3 and H-5).

**$^{13}$C NMR** (62.5 MHz, DMSO-$d_6$) δ 157.39, 155.37, 151.43, 147.05, 143.60, 137.94, 133.89, 131.69, 131.48, 130.97, 130.01, 129.13 (2C), 128.93 (2C), 124.26, 123.19, 121.30, 120.83, 120.35, 119.63, 116.44, 112.85.

#### 4.3.4. Synthesis of 3-(2-(2-chlorophenyl)benzofuro[3,2-b]pyridin-4-yl)phenol (**9**)

The compound was synthesized as described in section 4.3 with **5e** (0.24 g, 1.0 mmol), dry ammonium acetate (0.77 g, 10.0 mmol), **2a** (0.36 g, 1.0 mmol) with glacial acetic acid (2 mL) to yield 0.14 g (36.5%) of a white solid.

TLC (ethyl acetate/*n*-hexane = 2:5 v/v) $R_f$ = 0.25; Mp: 271.8–272.4 °C; HPLC: Retention time: 7.99 min, purity: 98.4%; ESI-MS: *m/z* calcd for $C_{23}H_{14}ClNO_2$ $[M+H]^+$: 372.08; found $[M+H]^+$: 372.22.

**$^1$H NMR** (250 MHz, DMSO-$d_6$) δ 9.86 (s, 1H, 4-phenyl 3-OH) 8.21

(d, $J$ = 7.65 Hz, 1H, benzofuro H-4), 7.89–7.85 (m, 2H, pyridine H-3 and benzofuro H-7), 7.76–7.49 (m, 8H, 2-phenyl H-3, H-4, H-5, H-6, 4-phenyl H-2, H-5, H-6 and benzofuro H-6), 7.41 (t, $J$ = 8.02 Hz, 1H, benzofuro H-5), 6.95 (d, $J$ = 7.90 Hz, 1H, 4-phenyl H-4).

**$^{13}$C NMR** (62.5 MHz, DMSO-$d_6$) δ 157.85, 157.11, 152.93, 145.51, 143.91, 138.86, 134.16, 132.01, 131.44, 130.25, 130.07, 129.85, 127.35, 124.12, 122.62, 121.09, 119.39, 116.74, 115.48, 112.56.

*4.3.5. Synthesis of 3-(2-(3-chlorophenyl)benzofuro[3,2-b]pyridin-4-yl)phenol (**10**)*

The compound was synthesized as described in section 4.3 with **5e** (0.24 g, 1.0 mmol), dry ammonium acetate (0.77 g, 10.0 mmol), **2b** (0.36 g, 1.0 mmol) with glacial acetic acid (2 mL) to yield 0.11 g (29.6%) of a whitish yellow solid.

TLC (ethyl acetate/$n$-hexane = 2:5 v/v) $R_f$ = 0.31; Mp: 223.9–224.5 °C; HPLC: Retention time: 8.88 min, purity: 100.0%; ESI-MS: $m/z$ calcd for $C_{23}H_{14}ClNO_2$ $[M+H]^+$: 372.08; found $[M+H]^+$: 372.55.

**$^1$H NMR** (250 MHz, DMSO-$d_6$) δ 9.87 (s, 1H, 4-phenyl 3-OH) 8.32–8.22 (m, 4H, 2-phenyl H-2, H-6, pyridine H-3 and benzofuro H-4), 7.82 (d, $J$ = 8.23 Hz, 1H, benzofuro H-7), 7.67 (t, $J$ = 7.5 Hz, 1H, benzofuro H-6), 7.58–7.48 (m, 5H, 2-phenyl H-4, H-5, 4-phenyl H-2, H-5 and H-6), 7.42 (t, $J$ = 7.62 Hz, 1H, benzofuro H-5), 6.97 (d, $J$ = 8.42 Hz, 1H, 4-phenyl H-4).

**$^{13}$C NMR** (62.5 MHz, DMSO-$d_6$) δ 158.09, 157.58, 151.83, 146.43, 144.45, 141.09, 134.65, 134.10, 132.83, 130.98, 130.49, 130.31, 128.96, 126.96, 125.97, 124.50, 122.96, 121.51, 120.03, 117.90, 117.06, 116.07, 112.91.

*4.3.6. Synthesis of 3-(2-(4-chlorophenyl)benzofuro[3,2-b]pyridin-4-yl)phenol (**11**)*

The compound was synthesized as described in section 4.3 with **5e** (0.48 g, 2 mmol), dry ammonium acetate (1.54 g, 20.0 mmol), **2c** (0.72 g, 2.0 mmol) with glacial acetic acid (5 mL) to yield 0.20 g (26.4%) of a pale yellow solid.

TLC (ethyl acetate/$n$-hexane = 2:5 v/v) $R_f$ = 0.31; Mp: 282.7–283.4 °C; HPLC: Retention time: 8.83 min, purity: 97.9%; ESI-MS: $m/z$ calcd for $C_{23}H_{14}ClNO_2$ $[M+H]^+$: 372.08; found $[M+H]^+$: 372.39.

**$^1$H NMR** (250 MHz, DMSO-$d_6$) δ 9.86 (s, 1H, 4-phenyl 3-OH) 8.34–8.22 (m, 4H, 2-phenyl H-2, H-6, pyridine H-3 and benzofuro H-4), 7.85 (d, $J$ = 8.25 Hz, 1H, benzofuro H-7), 7.69 (t, $J$ = 7.3 Hz, 1H, benzofuro H-6), 7.60–7.50 (m, 5H, 2-phenyl H-3, H-5, 4-phenyl H-2, H-5 and H-6), 7.43 (t, $J$ = 7.87 Hz, 1H, benzofuro H-5), 6.97 (d, $J$ = 8.07 Hz, 1H, 4-phenyl H-4).

**$^{13}$C NMR** (62.5 MHz, DMSO-$d_6$) δ 157.78, 157.22, 151.88, 145.94, 144.07, 137.50, 134.37, 133.69, 132.46, 130.10, 129.84, 128.73 (2C), 128.71 (2C), 124.07, 122.71, 121.04, 119.57, 117.25, 116.67, 115.70, 112.56.

*4.3.7. Synthesis of 4-(2-(2-chlorophenyl)benzofuro[3,2-b]pyridin-4-yl)phenol (**12**)*

The compound was synthesized as described in section 4.3 with **5f** (0.48 g, 2.0 mmol), dry ammonium acetate (1.54 g, 20.0 mmol), **2a** (0.72 g, 2.0 mmol) with glacial acetic acid (5 mL) to yield 86 mg (11.6%) of a yellow solid.

TLC (ethyl acetate/$n$-hexane = 2:5 v/v) $R_f$ = 0.29; Mp: 195.6–196.1 °C; HPLC: Retention time: 8.25 min, purity: 98.63%; ESI-MS: $m/z$ calcd for $C_{23}H_{14}ClNO_2$ $[M+H]^+$: 372.08; found $[M+H]^+$: 372.44.

**$^1$H NMR** (250 MHz, DMSO-$d_6$) δ 9.98 (s, 1H, 4-phenyl 4-OH), 8.2 (d, $J$ = 7.6 Hz, 1H, benzofuro H-4), 8.02 (d, 2H, d, $J$ = 8.6 Hz, 2H, 4-phenyl H-2 and H-6), 7.89–7.85 (m, 2H, pyridine H-3 and benzofuro H-7), 7.75–7.46 (m, 6H, 2-phenyl H-3, H-4, H-5, H-6, benzofuro H-5 and H-6), 7.01 (d, $J$ = 8.65 Hz, 2H, 4-phenyl H-3 and H-5).

**$^{13}$C NMR** (62.5 MHz, DMSO-$d_6$) δ 159.01, 156.99, 153.01, 145.31, 143.68, 139.10, 131.91, 131.47, 131.35, 130.21 (2C), 129.94, 129.77, 129.65, 127.26, 124.00, 123.36, 122.70, 120.96, 120.17, 115.99 (2C), 112.53.

*4.3.8. Synthesis of 4-(2-(3-chlorophenyl)benzofuro[3,2-b]pyridin-4-yl)phenol (**13**)*

The compound was synthesized as described in section 4.3 with **5f** (0.71 g, 3.0 mmol), dry ammonium acetate (2.31 g, 30.0 mmol), **2b** (1.08 g, 3.0 mmol) with glacial acetic acid (5 mL) to yield 0.10 g (8.9%) of a yellow solid.

TLC (ethyl acetate/$n$-hexane = 2:5 v/v) $R_f$ = 0.33; Mp: 270.5–271.1 °C; HPLC: Retention time: 9.07 min, purity: 98.7%; ESI-MS: $m/z$ calcd for $C_{23}H_{14}ClNO_2$ $[M+H]^+$: 372.08; found $[M+H]^+$: 372.42.

**$^1$H NMR** (250 MHz, DMSO-$d_6$) δ 10.09 (s, 1H, 4-phenyl 4-OH), 8.34 (br, 1H, benzofuro H-4), 8.27–8.19 (m, 3H, 2-phenyl H-2, H-6 and pyridine H-3), 8.1 (d, $J$ = 8.67 Hz, 2H, 4-phenyl H-2 and H-6), 7.83 (d, $J$ = 8.25 Hz, 1H, benzofuro H-7), 7.67 (td, $J$ = 7.2, 1.25 Hz, 1H, benzofuro H-6), 7.58–7.48 (m, 3H, 2-phenyl H-3, H-5 and benzofuro H-5), 7.01 (d, $J$ = 8.7 Hz, 2H, 4-phenyl H-3 and H-5).

**$^{13}$C NMR** (62.5 MHz, DMSO-$d_6$) δ 159.30, 157.43, 151.80, 146.22, 144.27, 141.23, 134.00, 132.60, 130.87, 130.78 (2C), 130.12, 128.80, 126.89, 125.89, 124.48, 123.84, 123.01, 121.38, 116.88, 116.18 (2C), 112.89.

*4.3.9. Synthesis of 4-(2-(4-chlorophenyl)benzofuro[3,2-b]pyridin-4-yl)phenol (**14**)*

The compound was synthesized as described in section 4.3 with **5f** (0.60 g, 2.5 mmol), dry ammonium acetate (1.93 g, 25.0 mmol), **2c** (1.08 g, 3.0 mmol) with glacial acetic acid (5 mL) to yield 0.14 g (14.7%) of a yellow solid.

TLC (ethyl acetate/$n$-hexane = 2:5 v/v) $R_f$ = 0.34; Mp: 285.8–286.2 °C; HPLC: Retention time: 9.03 min, purity: 100.0%; ESI-MS: $m/z$ calcd for $C_{23}H_{14}ClNO_2$ $[M+H]^+$: 372.08; found $[M+H]^+$: 372.13.

**$^1$H NMR** (250 MHz, DMSO-$d_6$) δ 10.06 (s, 1H, 4-phenyl 4-OH), 8.31 (d, $J$ = 8.52 Hz, 2H, 2-phenyl H-2 and H-6), 8.24–8.21 (m, 2H, benzofuro H-4 and pyridine H-3), 8.08 (d, $J$ = 8.60 Hz, 2H, 4-phenyl H-2 and H-6), 7.83 (d, $J$ = 8.22 Hz, 1H, benzofuro H-7), 7.66 (t, $J$ = 7.3 Hz, 1H, benzofuro H-6), 7.59–7.47 (m, 3H, benzofuro H-5, 2-phenyl H-3 and H-5), 7.01 (d, $J$ = 8.57 Hz, 2H, 4-phenyl H-3 and H-5).

**$^{13}$C NMR** (62.5 MHz, DMSO-$d_6$) δ 159.28, 157.38, 152.09, 146.06, 144.19, 137.92, 133.88, 132.54, 131.43 (2C), 130.72 (2C), 129.03, 128.97 (2C), 124.29, 123.87, 123.05, 121.28, 116.63, 116.17 (2C), 112.85.

*4.3.10. Synthesis of 2-(4-(2-chlorophenyl)benzofuro[3,2-b]pyridin-2-yl)phenol (**15**)*

The compound was synthesized as described in section 4.3 with **5a** (0.51 g, 2.0 mmol), dry ammonium acetate (1.54 g, 20.0 mmol), **2d** (0.85 g, 2.5 mmol) with glacial acetic acid (5 mL) to yield 0.24 g (32.8%) of a yellow solid.

TLC (ethyl acetate/$n$-hexane = 1:20 v/v) $R_f$ = 0.20; Mp: 189.9–190.5 °C; HPLC: Retention time: 7.63 min, purity: 97.7%; ESI-MS: $m/z$ calcd for $C_{23}H_{14}ClNO_2$ $[M+H]^+$: 372.08; found $[M+H]^+$: 372.37.

**$^1$H NMR** (250 MHz, $CDCl_3$) δ 14.02 (s, 1H, 2-phenyl 2-OH), 8.21 (d, $J$ = 7.6 Hz, 1H, benzofuro H-4), 8.01 (s, 1H, pyridine H-3), 7.86 (dd, $J$ = 8.02, 1.47 Hz, 1H, benzofuro H-7), 7.65–7.43 (m, 7H, benzofuro H-5, H-6, 2-phenyl H-6, 4-phenyl H-3, H-4, H-5 and H-6), 7.32 (td, $J$ = 7.07, 1.55 Hz, 1H, 2-phenyl H-5), 7.09 (dd, $J$ = 8.22, 1.2 Hz, 1H, 2-phenyl H-3), 6.9 (td, $J$ = 8.07, 1.27 Hz, 1H, 2-phenyl H-4).

**$^{13}$C NMR** (62.5 MHz, $CDCl_3$) δ 159.50, 158.09, 154.03, 146.48, 141.38, 133.48, 133.19, 133.00, 131.72, 131.42, 130.93, 130.62, 130.10, 127.42, 126.95, 124.25, 122.49, 121.56, 119.80, 119.43, 119.09, 118.85, 112.82.

#### 4.3.11. Synthesis of 3-(4-(2-chlorophenyl)benzofuro[3,2-b]pyridin-2-yl)phenol (**16**)

The compound was synthesized as described in section 4.3 with **5a** (0.77 g, 3.0 mmol), dry ammonium acetate (2.31 g, 30.0 mmol), **2e** (1.36 g, 4.0 mmol) with glacial acetic acid (5 mL) to yield 0.22 g (20.1%) of a white solid.

TLC (ethyl acetate/*n*-hexane = 2:5 v/v) $R_f$ = 0.32; Mp: 210.2–210.9 °C; HPLC: Retention time: 7.66 min, purity: 99.1%; ESI-MS: *m/z* calcd for $C_{23}H_{14}ClNO_2$ $[M+H]^+$: 372.08; found $[M+H]^+$: 372.82.

**$^1$H NMR** (250 MHz, $CDCl_3$) δ 8.34 (d, *J* = 7.82 Hz, 1H, benzofuro H-4), 7.82–7.79 (m, 2H, 2-phenyl H-2 and pyridine H-3), 7.62–7.37 (m, 8H, benzofuro H-5, H-6, H-7, 2-phenyl H-6, 4-phenyl H-3, H-4, H-5 and H-6), 7.32 (t, *J* = 7.8 Hz, 1H, 2-phenyl H-5), 6.89 (dd, *J* = 8.02, 2.47 Hz, 1H, 2-phenyl H-4).

**$^{13}$C NMR** (62.5 MHz, $CDCl_3$) δ 158.13, 156.90, 153.86, 147.04, 144.69, 141.16, 133.50, 133.45, 131.76, 131.64, 130.62, 130.51, 130.32, 129.65, 127.27, 123.97, 123.51, 122.01, 120.83, 119.71.116.39, 114.93, 112.51.

#### 4.3.12. Synthesis of 4-(4-(2-chlorophenyl)benzofuro[3,2-b]pyridin-2-yl)phenol (**17**)

The compound was synthesized as described in section 4.3 with **5a** (0.77, 3.0 mmol), dry ammonium acetate (2.30 g, 30.0 mmol), **2f** (1.36 g, 4.0 mmol) with glacial acetic acid (5 mL) to yield 0.12 g (12.3%) of a yellow solid.

TLC (ethyl acetate/*n*-hexane = 2:5 v/v) $R_f$ = 0.29; Mp: 260.1–260.7 °C; HPLC: Retention time: 6.88 min, purity: 97.1%; ESI-MS: *m/z* calcd for $C_{23}H_{14}ClNO_2$ $[M+H]^+$: 372.08; found $[M+H]^+$: 372.98.

**$^1$H NMR** (250 MHz, DMSO-$d_6$) δ 9.87 (s, 1H, 2-phenyl 4-OH), 8.25 (d, *J* = 7.65 Hz, 1H, benzofuro H-4), 8.06 (d, *J* = 8.47 Hz, 2H, 2-phenyl H-2 and H-6), 7.91 (s, 1H, pyridine H-3), 7.74–7.47 (m, 7H, benzofuro H-5, H-6, H-7, 4-phenyl H-3, H-4, H-5 and H-6), 6.89 (d, *J* = 8.5 Hz, 2H, 2-phenyl H-3 and H-5).

**$^{13}$C NMR** (62.5 MHz, DMSO-$d_6$) δ 158.82, 157.53, 153.57, 145.99, 143.55, 138.30, 133.31, 132.57, 132.25, 131.41, 130.26, 130.17, 129.86, 128.82 (2C), 1.28.13, 124.51, 123.28, 121.47, 119.08, 116.07 (2C), 112.97.

#### 4.3.13. Synthesis of 2-(4-(3-chlorophenyl)benzofuro[3,2-b]pyridin-2-yl)phenol (**18**)

The compound was synthesized as described in section 4.3 with **5b** (0.77 g, 3.0 mmol), dry ammonium acetate (2.31 g, 30.0 mmol), **2d** (1.36 g, 4.0 mmol) with glacial acetic acid (5 mL) to yield 0.22 g (20.1%) of a white solid.

TLC (ethyl acetate/*n*-hexane = 1:20 v/v) $R_f$ = 0.21; Mp: 173.8–174.4 °C; HPLC: Retention time: 12.20 min, purity: 98.1%; ESI-MS: *m/z* calcd for $C_{23}H_{14}ClNO_2$ $[M]^+$: 371.07; found $[M]^+$: 371.4.

**$^1$H NMR** (250 MHz, DMSO-$d_6$) δ 13.02 (br s, 1H, 2-phenyl 2-OH), 8.37 (s, 1H, pyridine H-3), 8.19–8.07 (m, 4H, benzofuro H-4, 2-phenyl H-6, 4-phenyl H-2 and H-6), 7.83 (d, *J* = 8.27 Hz, 1H, benzofuro H-7), 7.71–7.63 (m, 3H, benzofuro H-6, 4-phenyl H-4 and H-5), 7.52 (t, *J* = 7.32 Hz, 1H, benzofuro H-5), 7.31 (t, *J* = 7.62 Hz, 1H, 2-phenyl H-5), 6.98–6.92 (m, 2H, 2-phenyl H-3 and H-4).

**$^{13}$C NMR** (62.5 MHz, DMSO-$d_6$) δ 158.06, 157.34, 153.92, 145.48, 141.57, 135.21, 134.13, 132.24, 132.19, 131.31, 131.23, 130.57, 130.05, 128.81, 128.67, 128.03, 124.70, 121.70, 121.15, 120.61, 119.53, 117.90, 113.03.

#### 4.3.14. Synthesis of 3-(4-(3-chlorophenyl)benzofuro[3,2-b]pyridin-2-yl)phenol (**19**)

The compound was synthesized as described in section 4.3 with **5b** (0.51 g, 2.0 mmol), dry ammonium acetate (1.54 g, 20.0 mmol), **2e** (0.85 g, 2.5 mmol) with glacial acetic acid (5 mL) to yield 0.26 g (33.8%) of a yellow solid.

TLC (ethyl acetate/*n*-hexane = 2:5 v/v) $R_f$ = 0.28; Mp: 220.9–221.5 °C; HPLC: Retention time: 8.92 min, purity: 97.9%; ESI-MS: *m/z* calcd for $C_{23}H_{14}ClNO_2$ $[M+H]^+$: 372.08; found $[M+H]^+$: 372.53.

**$^1$H NMR** (250 MHz, DMSO-$d_6$) δ 9.52 (br s, 1H, 2-phenyl 3-OH), 8.26–8.11 (m, 4H, benzofuro H-4, 4-phenyl H-2, H-6 and pyridine H-3), 7.85 (d, *J* = 8.25 Hz, 1H, benzofuro H-7), 7.72–7.63 (m, 5H, benzofuro H-6, 2-phenyl H-2, H-6, 4-phhenyl H-4 and H-5), 7.53 (td, *J* = 7.9, 0.77 Hz, 1H, benzofuro H-5), 7.33 (t, *J* = 7.87 Hz, 1H, 2-phenyl H-5), 6.89–6.85 (m, 1H, 2-phenyl H-4).

**$^{13}$C NMR** (62.5 MHz, DMSO-$d_6$) δ 157.96, 157.43, 153.69, 145.68, 144.24, 140.19, 135.59, 134.03, 131.06, 130.77, 130.01, 129.90, 129.63, 128.63, 127.83, 124.35, 122.94, 121.14, 118.19, 117.59, 116.15, 114.10, 112.85.

#### 4.3.15. Synthesis of 4-(4-(3-chlorophenyl)benzofuro[3,2-b]pyridin-2-yl)phenol (**20**)

The compound was synthesized as described in section 4.3 with **5b** (0.51 g, 2.0 mmol), dry ammonium acetate (1.54 g, 20.0 mmol), **2f** (0.85 g, 2.5 mmol) with glacial acetic acid (5 mL) to yield 0.11 g (23.5%) of a yellow solid.

TLC (ethyl acetate/*n*-hexane = 2:5 v/v) $R_f$ = 0.28; Mp: 241.6–242.1 °C; HPLC: Retention time: 8.09 min, purity: 99.9%; ESI-MS: *m/z* calcd for $C_{23}H_{14}ClNO_2$ $[M]^+$: 371.07; found $[M]^+$: 371.49.

**$^1$H NMR** (250 MHz, DMSO-$d_6$) δ 9.82 (br s, 1H, 2-phenyl 4-OH), 8.25–8.09 (m, 6H, benzofuro H-4, 2-phenyl H-2, H-6, 4-phenyl H-2, H-6 and pyridine H-3), 7.84 (d, *J* = 8.25 Hz, 1H, benzofuro H-7), 7.69–7.60 (m, 3H, benzofuro H-6, 4-phenyl H-4 and H-5), 7.51 (t, *J* = 7.22 Hz, 1H, benzofuro H-5), 6.91 (d, *J* = 8.67 Hz, 2H, 2-phenyl H-3 and H-5).

**$^{13}$C NMR** (62.5 MHz, DMSO-$d_6$) δ 158.72, 157.39, 153.93, 145.42, 144.09, 135.81, 134.11, 131.16, 130.86, 129.94, 129.83, 129.69, 128.81 (2C), 128.70, 127.94, 124.34, 123.11, 121.26, 116.63, 115.77 (2C), 112.92.

#### 4.3.16. Synthesis of 2-(4-(4-chlorophenyl)benzofuro[3,2-b]pyridin-2-yl)phenol (**21**)

The compound was synthesized as described in section 4.3 with **5c** (0.51 g, 2.0 mmol), dry ammonium acetate (1.54 g, 20.0 mmol), **2d** (0.85 g, 2.5 mmol) with glacial acetic acid (5 mL) to yield 0.17 g (23.4%) of a yellow solid.

TLC (ethyl acetate/*n*-hexane = 1:20 v/v) $R_f$ = 0.23; Mp: 188.9–189.5 °C; HPLC: Retention time: 9.74 min, purity: 97.2%; ESI-MS: *m/z* calcd for $C_{23}H_{14}ClNO_2$ $[M+H]^+$: 372.08; found $[M+H]^+$: 372.26.

**$^1$H NMR** (250 MHz, $CDCl_3$) δ 13.95 (s, 1H, 2-phenyl 2-OH), 8.16 (d, *J* = 7.67 Hz, 1H, benzofuro H-4), 8.04 (s, 1H, pyridine H-3), 7.96 (d, *J* = 8.45 Hz, 2H, 4-phebyl H-2 and H-6), 7.88 (d, *J* = 8.0 Hz, 1H, benzofuro H-7), 7.64–7.54 (m, 4H, benzofuro H-6, 2-phenyl H-6, 4-phenyl H-3 and H-5), 7.45 (td, *J* = 7.75, 1.5 Hz, 1H, benzofuro H-5), 7.32 (td, *J* = 8.2, 1.05 Hz, 1H, 2-phenyl H-5), 7.07 (d, *J* = 8.05 Hz, 1H, 2-phenyl H-3), 6.94 (t, *J* = 7.8 Hz, 1H, 2-phenyl H-4).

**$^{13}$C NMR** (62.5 MHz, $CDCl_3$) δ 159.52, 158.01, 154.60, 146.00, 141.83, 136.31, 133.31, 132.30, 131.47, 130.41 (2C), 130.13, 129.67 (2C), 126.81, 124.33, 122.32, 121.58, 119.73, 119.41, 118.91, 116.10, 112.73.

*4.3.17. Synthesis of 3-(4-(4-chlorophenyl)benzofuro[3,2-b]pyridin-2-yl)phenol (**22**)*

The compound was synthesized as described in section 4.3 with **5c** (0.51 g, 2.0 mmol), dry ammonium acetate (1.54 g, 20.0 mmol), **2e** (0.85 g, 2.5 mmol) with glacial acetic acid (5 mL) to yield 0.22 mg (29.1%) of a pale yellow solid.

TLC (ethyl acetate/*n*-hexane = 2:5 v/v) $R_f$ = 0.34; Mp: 223.7–224.3 °C; HPLC: Retention time: 8.26 min, purity: 96.7%; ESI-MS: *m/z* calcd for $C_{23}H_{14}ClNO_2$ $[M+H]^+$: 372.08; found $[M+H]^+$: 372.33.

**$^1$H NMR** (250 MHz, DMSO-$d_6$) δ 9.65 (s, 1H, 2-phenyl 3-OH), 8.26–8.18 (m, 4H, benzofuro H-4, 4-phenyl H-2, H-6 and pyridine H-3), 7.84 (d, *J* = 8.3 Hz, 1H, benzofuro H-7), 7.71–7.64 (m, 5H, benzofuro H-6, 2-phenyl H-2, H-6, 4-phhenyl H-3 and H-5), 7.53 (t, *J* = 7.57, Hz, 1H, benzofuro H-5), 7.33 (t, *J* = 7.75 Hz, 1H, 2-phenyl H-5), 6.87 (dd, 1H, *J* = 6.77, 2.3 Hz, 1H, 2-phenyl H-4).

**$^{13}$C NMR** (62.5 MHz, DMSO-$d_6$) δ 158.05, 157.47, 153.71, 145.93, 144.28, 140.30, 134.77, 132.38, 131.05, 130.97 (2C), 130.11, 130.06, 129.39 (2C), 124.45, 123.01, 121.28, 118.21, 117.48, 116.22, 114.11, 112.92.

*4.3.18. Synthesis of 4-(4-(4-chlorophenyl)benzofuro[3,2-b]pyridin-2-yl)phenol (**23**)*

The compound was synthesized as described in section 4.3 with **5c** (0.62 g, 2.5 mmol), dry ammonium acetate (1.93 g, 25.0 mmol), **2f** (1.02 g, 3.0 mmol) with glacial acetic acid (5 mL) to yield 0.15 g (16.2%) of a yellow solid.

TLC (ethyl acetate/*n*-hexane = 2:5 v/v) $R_f$ = 0.30; Mp: 285.2–286.1 °C; HPLC: Retention time: 8.27 min, purity: 96.1%; ESI-MS: *m/z* calcd for $C_{23}H_{14}ClNO_2$ $[M+H]^+$: 372.08; found $[M+H]^+$: 372.56.

**$^1$H NMR** (250 MHz, DMSO-$d_6$) δ 9.82 (s, 1H, 2-phenyl 4-OH), 8.25–8.11 (m, 6H, benzofuro H-4, 2-phenyl H-2, H-6, 4-phenyl H-2, H-6 and pyridine H-3), 7.81 (d, *J* = 8.25 Hz, 1H, benzofuro H-7), 7.7–7.62 (m, 3H, benzofuro H-6, 4-phenyl H-3 and H-5), 7.51 (t, *J* = 7.42 Hz, 1H, benzofuro H-5), 6.91 (d, *J* = 8.67 Hz, 2H, 2-phenyl H-3 and H-5).

**$^{13}$C NMR** (62.5 MHz, DMSO-$d_6$) δ 158.72, 157.39, 153.96, 145.44, 144.11, 134.72, 132.55, 131.10, 130.95 (2C), 129.96, 129.90, 129.40 (2C), 128.78 (2C), 124.35, 123.15, 121.30, 116.44, 115.82 (2C), 112.87.

### 4.4. Pharmacology

*4.4.1. DNA topoisomerase I and II relaxation assay*

All the test compounds were dissolved in DMSO at a concentration of 20 mM as a stock solution and stored under −20 °C until needed. The DNA topoisomerase I and II inhibitory activity of each compound was measured as follows according to the manufacturer's protocol. A mixture comprising of 100 ng supercoiled pBR322 plasmid DNA (Thermo Scientific, USA) and 1 unit of recombinant human DNA topo I (TopoGEN INC., USA) or topo II (Usb Corp., USA) was incubated with and without the prepared compounds in the assay buffer (For topo I, 10 mM Tris-HCl (pH 7.9) containing 150 mM NaCl, 0.1% bovine serum albumin (BSA), 0.1 mM spermidine and 5% glycerol; For topo II, 10 mM Tris-HCl (pH 7.9) containing 50 mM NaCl, 50 mM KCl, 5 mM $MgCl_2$, 1 mM EDTA, 1 mM ATP and 15 μg/mL BSA) for 30 min at 37 °C. The reaction in a final volume of 10 μL was quenched by adding 1 μL of the stop solution (For topo I, 10% SDS solution containing 0.2% bromophenol blue, 0.2% xylene cyanol and 30% glycerol; for topo II, 7 mM EDTA). The reaction products were analyzed on 0.8% agarose gel at 50 V for 1 h with TAE as the running buffer. The gels were stained in an EtBr solution (0.5 μg/mL). DNA bands were visualized by trans-illumination with UV light and were quantitated using Alpha Tech Imager (Alpha Innotech Corporation). To analyze the effect of compound **14** on intracellular topo-mediated DNA relaxation in vivo, we prepared nuclear fractionations of compound-treated and untreated cells according to the method reported previously [31]. The DNA relaxation activity of the prepared nuclear extract was defined through the determination of the amount of each nuclear extraction product that could completely relax 100 ng pBR322 DNA (Fermentas, USA) by incubating at 37 °C for 20 min. The DNA reacted with nuclear extract was separated via electrophoresis on a 1.0% agarose gel at 50 V for 50 min with TAE as the running buffer. The gel staining and DNA band visualizing were performed as the same method used for recombinant DNA topo I and II *in vitro* relaxation assay.

*4.4.2. kDNA decatenation assay*

The assay was performed by the method previously published [31]. kDNA 75 ng was added in the reaction buffer containing 50 mM Tris-HCl (pH 8.0), 120 mM KCl, 10 mM MgCl2, 0.5 mM dithiothreitol, 0.5 mM ATP, 30 μg/mL bovine serum albumin followed by addition of compound as designated concentration in figure legend. A total reaction volume was 10 μL. Reactions were initiated by the addition of 3 units of topo II, and mixtures were incubated for 30 min at 37 °C. The reaction was terminated by the addition of 2.5 μL of stock solution (5% SDS, 25% ficoll, and 0.05% bromphenol blue) followed by treatment with 0.25 mg/ml proteinase K (Sigma, USA) at 37 °C for 30 min to eliminate the protein. Samples were resolved by electrophoresis on a 1.2% (w/v) agarose gel containing 0.5 μg/ml ethidium bromide in TAE buffer (100 mM Tris-acetate and 2 mM Na2EDTA, pH 8.3). DNA bands were visualized as followed DNA topo II relaxation assay.

*4.4.3. Antiproliferative assay*

Cancer cells were cultured according to the supplier's instructions. Cells were seeded in 96-well plates at a density of 2–4 x $10^4$ cells per well with incubation for overnight in 0.1 mL of media supplied with 10% fetal bovine serum (FBS, Hyclone, USA) in 5% $CO_2$ incubator at 37 °C. After FBS starvation for 4 h, culture medium in each well was exchanged with 0.1 mL aliquots of medium containing graded concentrations of compounds followed by additional incubation for 72 h. Then each well was added with 5 μL of the cell counting kit-8 solution (Dojindo, Japan) followed by additional incubation for 4 h under the same condition. The absorbance of each well was determined by an Automatic Elisa Reader System (Bio-Rad 3550) at 450 nm wavelength. For determination of the $IC_{50}$ values, the absorbance readings at 450 nm were fitted to the four-parameter logistic equation using Table Curve 2D (SPSS Inc., USA). The reference compounds such as adriamycin, etoposide and camptothecin were purchased from Sigma (USA).

*4.4.4. Cleavable complex assay*

The mixture of 250 ng of supercoiled DNA pBR322 and 3 units of human topoisomerase II with or without compound at the designated concentrations in the figure legend was incubated at 37 °C for 30 min in the topo II relaxation assay buffer. The reaction was then terminated by the addition of 2.5 μL of stop solution (5% SDS, 25% ficoll and 0.05% bromophenol blue) followed by treatment of 2 μL of 0.25 mg/mL proteinase K (Sigma, USA) with continuous incubation at 45 °C for 30 min to eliminate the protein. Samples were electrophoresed on a 1% (w/v) agarose gel containing 0.5 μg/mL EtBr at 30 V for 6 h in TAE running buffer. DNA bands on the gel were detected by UV and visualized by AlphaImager™.

*4.4.5. Band depletion assay*

HCT15 cells were seeded overnight at a density of 2 × $10^5$ cells per well. The cells were treated for 2 h at 37 °C with each of etoposide and compound **14**, and co-treated with etoposide and

compound **14** followed by cell harvesting. The cell pellet after centrifugation (4 °C, 3200 rpm, and 3 min) was washed with 1 mL of PBS and then ice-incubated for 1.5 h, followed by lysis with denaturing agent (62.5 mM Tris-HCl (pH 6.8), 1 mM EDTA and 2% SDS) and sonication (10–20 bursts, 2 s). The samples were ice-incubated for 20 min and centrifuged for 20 min (4 °C and 12,000 rpm) again. Finally the supernatant of sample was taken to perform Western blot analysis on 10% SDS-PAGE gels.

*4.4.6. Comet assay*

To evaluate DNA damage, comet assay was performed using single-cell gel electrophoresis with a Trevigen kit (Gaithersburg, USA) according to the method previously reported [43]. Briefly, HCT15 cells, seeded in a density of $1 \times 10^5$ cells per well in six-well plates were treated with compound **14** and etoposide for 24 h at the designated concentration in figure legend and harvested by trypsinization followed by resuspending cells in 1 mL of ice-cold PBS. Then, 8 μL of resuspened cells were mixed with 80 μL of low-melting agarose at 37 °C, spread on slides and solidified in the dark for 40 min at 4 °C. Slides were lysed in ice-cold lysis solution in the dark for 30 min at 4 °C and then submerged in a fresh alkaline solution (pH > 13) at room temperature for 30 min to allow alkaline unwinding. Electrophoresis was performed under alkaline conditions for 20 min for 15 V. Slides were rinsed twice with distilled water, once with 70% ethanol and stained with SYBR Green (Trevigen INC., USA) in a TE buffer for 5 min in the dark at 4 °C. Comet images were obtained using an inverted fluorescence microscope (Zeiss, Axiovert 200) at 10× magnification and percent DNA in tail was analyzed by Komet 5.0 software (Kinetic imaging Ltd, UK). Data were represented both by imaging and graphically by randomly selecting comet lengths of HCT15 cells.

*4.4.7. Competitive EtBr displacement assay*

ctDNA (30 μM) was mixed with EtBr (20 μM) in the 10 mM tris buffer solution (pH 7.2), followed by incubation for 30 min at room temperature with shaking. Each compound (m-AMSA and compound **14**) was added to the well containing the mixture of EtBr and ctDNA with increased concentrations up to 40 μM as designated in the figure legend. The DMSO was added for untreated control in the same amount as compound addition and the final DMSO amount was equally 1% for all samples. After addition of compound, the plate was continuously incubated for 30 min at room temperature with shaking. The fluorescence intensity of EtBr was measured by TECAN multimode microplate reader (Swizerland) with excitation at 471 nm. The emission spectrum was collected at 500–700 nm.

*4.4.8. Western blotting*

HCT15 cells were grown on 60 mm tissue culture dishes at $1 \times 10^6$ cells until reaching 80% confluency. The cells were then treated with compound **14** in concentrations of 10 and 30 μM for 24 h followed by lysis with a lysis buffer solution containing 50 mM Tris HCl, 300 mM NaCl, 1% Triton X-100, 10% glycerol, 1.5 mM $MgCl_2$, 1 mM $CaCl_2$, 1 mM PMSF and 1% protease inhibitor cocktail. 60 μg of protein per sample was resolved by 12% SDS-PAGE and transferred to a PVDF membrane (Millipore, USA). The membranes were blocked with 5% skim milk in Tris buffered saline containing 0.1% tween 20 (TBST) and probed with primary antibodies in a dilution ratio of 1:1000 for 2–3 h. The blots were washed, exposed to HRP-conjugated anti-rabbit IgG (Cell Signaling Technology Inc. USA) in a dilution ratio of 1:2000 for 2 h, and detected with ECL western blotting detection reagent (Animal genetics Inc, Korea). All primary antibodies used were purchased from Cell Signaling Technology Inc. (USA). Western blot images were taken by LAS-3000 (Fuji Photo Film Co., Ltd, Japan) and analyzed using Multi-Gauge Software (Fuji Photo Film Co. Ltd., Japan).

## Acknowledgements

This research was supported by the Basic Science Research Program through the National Research Foundation of Korea (NRF) funded by the Ministry of Education, Science and Technology (NRF-2015R1A2A1A15054445 and NRF-2013R1A1A2060408) and by the Korean Health Technology R&D Project funded by Ministry of Health & Welfare, Republic of Korea (HI14C2469).

## Appendix A. Supplementary data

Supplementary data related to this article can be found at http://dx.doi.org/10.1016/j.ejmech.2017.01.003.

## References

[1] G.I. Evan, K.H. Vousden, Proliferation, cell cycle and apoptosis in cancer, Nature 411 (2001) 342–348.
[2] S.Z. Millis, S. Ejadi, M.J. Demeure, Molecular profiling of refractory adrenocortical cancers and predictive biomarkers to therapy, Biomark. Cancer 7 (2015) 69–76.
[3] J.C. Wang, Cellular roles of DNA topoisomerases: a molecular perspective, Nat. Rev. Mol. Cell Biol. 3 (2002) 430–440.
[4] J.C. Wang, DNA topoisomerases, Annu. Rev. Biochem. 65 (1996) 635–692.
[5] J.C. Wang, DNA topoisomerases, Annu. Rev. Biochem. 54 (1985) 665–697.
[6] A.Y. Chen, L.F. Liu, DNA Topoisomerases: essential enzymes and lethal targets, Annu. Rev. Pharmacol. Toxicol. 34 (1994) 191–218.
[7] P. Forterre, S. Gribaldo, D. Gadelle, M.-C. Serre, Origin and evolution of DNA topoisomerases, Biochimie 89 (2007) 427–446.
[8] J.L. Nitiss, Targeting DNA topoisomerase II in cancer chemotherapy, Nat. Rev. Cancer 9 (2009) 338–350.
[9] M. Li, Y. Liu, Topoisomerase I in human disease pathogenesis and treatments, Genomics Proteomics Bioinforma. 14 (2016) 166–171.
[10] D. Gewirtz, A critical evaluation of the mechanisms of action proposed for the antitumor effects of the anthracycline antibiotics adriamycin and daunorubicin, Biochem. Pharmacol. 57 (1999) 727–741.
[11] I. Husain, J.L. Mohler, H.F. Seigler, J.M. Besterman, Elevation of topoisomerase I messenger RNA, protein, and catalytic activity in human tumors: demonstration of tumor-type specificity and implications for cancer chemotherapy, Cancer Res. 54 (1994) 539–546.
[12] J.A. Holden, D.H. Rolfson, C.T. Wittwer, Human DNA topoisomerase II: evaluation of enzyme activity in normal and neoplastic tissues, Biochem. (Mosc.) 29 (1990) 2127–2134.
[13] M.M. Heck, W.N. Hittelman, W.C. Earnshaw, Differential expression of DNA topoisomerases I and II during the eukaryotic cell cycle, Proc. Natl. Acad. Sci. 85 (1988) 1086–1090.
[14] C.M. Whitacre, E. Zborowska, N.H. Gordon, W. Mackay, N.A. Berger, Topotecan increases topoisomerase IIα levels and sensitivity to treatment with etoposide in schedule-dependent process, Cancer Res. 57 (1997) 1425–1428.
[15] W.A. Denny, Emerging DNA topoisomerase inhibitors as anticancer drugs, Expert Opin. Emerg. Drugs 9 (2004) 105–133.
[16] S. Wang, W. Miller, J. Milton, N. Vicker, A. Stewart, P. Charlton, P. Mistry, D. Hardick, W.A. Denny, Structure–activity relationships for analogues of the phenazine-based dual topoisomerase I/II inhibitor XR11576, Bioorg. Med. Chem. Lett. 12 (2002) 415–418.
[17] C. Palma, M. Criscuoli, A. Lippi, M. Muratori, S. Mauro, C.A. Maggi, Effect of the aromatase inhibitor, MEN 11066, on growth of two different MCF-7 sublines, Eur. J. Pharmacol. 409 (2000) 93–101.
[18] Y. Xia, Y. Jin, N. Kaur, Y. Choi, K. Lee, HIF-1α inhibitors: synthesis and biological evaluation of novel moracin O and P analogues, Eur. J. Med. Chem. 46 (2011) 2386–2396.
[19] K. Suzuki, T. Okawara, T. Higashijima, K. Yokomizo, T. Mizushima, M. Otsuka, Inhibitory activities against topoisomerase I and II by isoaurostatin derivatives and their structure–activity relationships, Bioorg. Med. Chem. Lett. 15 (2005) 2065–2068.
[20] K. Asoh, M. Kohchi, I. Hyoudoh, T. Ohtsuka, M. Masubuchi, K. Kawasaki, H. Ebiike, Y. Shiratori, T.A. Fukami, O. Kondoh, T. Tsukaguchi, N. Ishii, Y. Aoki, N. Shimma, M. Sakaitani, Synthesis and structure–activity relationships of novel benzofuran farnesyltransferase inhibitors, Bioorg. Med. Chem. Lett. 19 (2009) 1753–1757.
[21] Y. Xiang, B. Hirth, G. Asmussen, H.-P. Biemann, K.A. Bishop, A. Good, M. Fitzgerald, T. Gladysheva, A. Jain, K. Jancsics, J. Liu, M. Metz, A. Papoulis, R. Skerlj, J.D. Stepp, R.R. Wei, The discovery of novel benzofuran-2-carboxylic acids as potent Pim-1 inhibitors, Bioorg. Med. Chem. Lett. 21 (2011) 3050–3056.
[22] J.J. Buggy, Z.A. Cao, K.E. Bass, E. Verner, S. Balasubramanian, L. Liu, B.E. Schultz, P.R. Young, S.A. Dalrymple, CRA-024781: a novel synthetic inhibitor of histone deacetylase enzymes with antitumor activity in vitro and in vivo, Am. Assoc. Cancer Res. 5 (2006) 1309–1317.
[23] I.N. Gaisina, F. Gallier, A.V. Ougolkov, K.H. Kim, T. Kurome, S. Guo, D. Holzle,

D.N. Luchini, S.Y. Blond, D.D. Billadeau, A.P. Kozikowski, From a natural product lead to the identification of potent and selective benzofuran-3-yl-(indol-3-yl)maleimides as glycogen synthase kinase 3β inhibitors that suppress proliferation and survival of pancreatic cancer cells, J. Med. Chem. 52 (2009) 1853–1863.
[24] C. Salomé, N. Ribeiro, T. Chavagnan, F. Thuaud, M. Serova, A. de Gramont, S. Faivre, E. Raymond, L. Désaubry, Benzofuran derivatives as anticancer inhibitors of mTOR signaling, Eur. J. Med. Chem. 81 (2014) 181–191.
[25] R. Wilcken, M.O. Zimmermann, A. Lange, A.C. Joerger, F.M. Boeckler, Principles and applications of halogen bonding in medicinal chemistry and chemical biology, J. Med. Chem. 56 (2013) 1363–1388.
[26] Z. Xu, Z. Yang, Y. Liu, Y. Lu, K. Chen, W. Zhu, Halogen bond: its role beyond drug–target binding affinity for drug discovery and development, J. Chem. Inf. Model 54 (2014) 69–78.
[27] M.O. Zimmermann, A. Lange, R. Wilcken, M.B. Cieslik, T.E. Exner, A.C. Joerger, P. Koch, F.M. Boeckler, Halogen-enriched fragment libraries as chemical probes for harnessing halogen bonding in fragment-based lead discovery, Future Med. Chem. 6 (2014) 617–639.
[28] T.M. Kadayat, S. Park, K.-Y. Jun, T.B.T. Magar, G. Bist, A. Shrestha, Y. Na, Y. Kwon, E.-S. Lee, Effect of chlorine substituent on cytotoxic activities: design and synthesis of systematically modified 2,4-diphenyl-5H-indeno[1,2-b]pyridines, Bioorg. Med. Chem. Lett. 26 (2016) 1726–1731.
[29] T.M. Kadayat, C. Song, Y. Kwon, E.-S. Lee, Modified 2,4-diaryl-5H-indeno[1,2-b]pyridines with hydroxyl and chlorine moiety: synthesis, anticancer activity, and structure–activity relationship study, Bioorg. Chem. 62 (2015) 30–40.
[30] R. Karki, K.-Y. Jun, T.M. Kadayat, S. Shin, T.B. Thapa Magar, G. Bist, A. Shrestha, Y. Na, Y. Kwon, E.-S. Lee, A new series of 2-phenol-4-aryl-6-chlorophenyl pyridine derivatives as dual topoisomerase I/II inhibitors: synthesis, biological evaluation and 3D-QSAR study, Eur. J. Med. Chem. 113 (2016) 228–245.
[31] H.-B. Kwon, C. Park, K.-H. Jeon, E. Lee, S.-E. Park, K.-Y. Jun, T.M. Kadayat, P. Thapa, R. Karki, Y. Na, M.S. Park, S.B. Rho, E.-S. Lee, Y. Kwon, A series of novel terpyridine-skeleton molecule derivants inhibit tumor growth and metastasis by targeting topoisomerases, J. Med. Chem. 58 (2015) 1100–1122.
[32] X. Xiao, M. Cushman, An Ab initio quantum mechanics calculation that correlates with ligand orientation and DNA cleavage site selectivity in camptothecin–DNA–topoisomerase I ternary cleavage complexes, J. Am. Chem. Soc. 127 (2005) 9960–9961.
[33] P. Thapa, Y. Jahng, P.-H. Park, J.-G. Jee, Y. Kwon, E.-S. Lee, 2,4-diaryl benzofuro [3,2-b]pyridine derivatives: design, synthesis, and evaluation of topoisomerase inhibitory activity and cytotoxicity, Bull. Korean Chem. Soc. 34 (2013) 3073–3082.
[34] F. KröHnke, The specific synthesis of pyridines and oligopyridines 1, Synthesis 1976 (1976) 1–24.
[35] S.J. Froelich-Ammon, N. Osheroff, Topoisomerase poisons: harnessing the dark side of enzyme mechanism, J. Biol. Chem. 270 (1995) 21429–21432.
[36] J.C. Marini, K.G. Miller, P.T. Englund, Decatenation of kinetoplast DNA by topoisomerases, J. Biol. Chem. 255 (1980) 4976–4979.
[37] B.B. Hasinoff, M.E. Abram, N. Barnabé, T. Khélifa, W.P. Allan, J.C. Yalowich, The catalytic DNA topoisomerase II inhibitor dexrazoxane (ICRF-187) induces differentiation and apoptosis in human leukemia K562 cells, Mol. Pharmacol. 59 (2001) 453–461.
[38] A. Ivashkevich, C.E. Redon, A.J. Nakamura, R.F. Martin, O.A. Martin, Use of the gamma-H2AX assay to monitor DNA damage and repair in translational cancer research, Cancer Lett. 327 (2012) 123–133.
[39] P. Majumdar, C. Bathula, S.M. Basu, S.K. Das, R. Agarwal, S. Hati, A. Singh, S. Sen, B.B. Das, Design, synthesis and evaluation of thiohydantoin derivatives as potent topoisomerase I (Top1) inhibitors with anticancer activity, Eur. J. Med. Chem. 102 (2015) 540–551.
[40] J.C. Reed, Balancing cell life and death: bax, apoptosis, and breast cancer, J. Clin. Invest 97 (1996) 2403–2404.
[41] A. Basu, S. Haldar, The relationship between BcI2, Bax and p53: consequences for cell cycle progression and cell death, Mol. Hum. Reprod. 4 (1998) 1099–1109.
[42] S.H. Kaufmann, S. Desnoyers, Y. Ottaviano, N.E. Davidson, G.G. Poirier, Specific proteolytic cleavage of poly(ADP-ribose) polymerase: an early marker of chemotherapy-induced apoptosis, Cancer Res. 53 (1993) 3976–3985.
[43] R.R. Tice, E. Agurell, D. Anderson, B. Burlinson, A. Hartmann, H. Kobayashi, Y. Miyamae, E. Rojas, J.C. Ryu, Y.F. Sasaki, Single cell gel/comet assay: guidelines for in vitro and in vivo genetic toxicology testing, Environ. Mol. Mutagen 35 (2000) 206–221.